

CP -violating observables in four-body $B \rightarrow \phi(\rightarrow K\bar{K})K^*(\rightarrow K\pi)$ decays

Chao-Qi Zhang¹, Jia-Ming Li¹, Meng-Kun Jia¹, Ya Li^{2,*} and Zhou Rui^{1†}

¹ College of Sciences, North China University of Science and Technology, Tangshan, Hebei 063210, China and

² Department of Physics, College of Science, Nanjing Agricultural University, Nanjing, Jiangsu 210095, China
(Dated: December 22, 2021)

We analyse the four-body $B \rightarrow \phi(\rightarrow K\bar{K})K^*(\rightarrow K\pi)$ decays in the perturbative QCD approach, where the invariant mass of $K\bar{K}$ ($K\pi$) system is limited in a window of ± 15 MeV (± 150 MeV) around the nominal $\phi(K^*(892))$ mass. In addition to the dominant P -wave resonances, two important S -wave backgrounds in the selected invariant mass region are also accounted for. Angular momentum conservation allows six helicity amplitudes to contribute, including three P -waves, two single S -waves, and one double S -wave, in the decays under study. We calculated the branching ratio for each component and found sizable S -wave contributions, which coincide roughly with the experimental observation. The obtained branching ratios of $B^{0(+)} \rightarrow \phi K^{*0(+)}$ are comparable with the previous theoretical predictions and support the experimental measurements, whereas the predicted $\mathcal{B}(B_s^0 \rightarrow \phi\bar{K}^{*0})$ is an order of magnitude smaller than the current world average in its central value. The longitudinal polarizations are predicted to be around 0.7, consistent with previous PQCD results but larger than the world average values. Aside from the direct CP asymmetries, the true and fake triple product asymmetries, originate from the interference between the perpendicular polarization amplitude and other helicity amplitudes, are also calculated in this work. In the special case of the neutral modes, both the direct CP asymmetries and true triple product asymmetries are expected to be zero due to the vanishing weak phase difference. The direct CP asymmetries for the B^+ mode are predicted to be tiny, of order 10^{-2} , since the tree contributions are suppressed strongly with respect to the penguin ones. The true triple product asymmetries have shown no significant deviations from zero. In contrast, large fake asymmetries are observed in these decays, indicating the presence of significant final-state interactions. We give the theoretical predictions of the S -wave induced triple product asymmetries for the first time, which is consistent with current LHCb data and would be checked with future measurements from Belle and BABAR experiments if the S -wave components can be properly taken into account in the angular analysis.

PACS numbers: 13.25.Hw, 12.38.Bx, 14.40.Nd

I. INTRODUCTION

The phenomenology of B decays to two light vector mesons provides unique opportunities for understanding the mechanism of hadronic weak decays and their CP asymmetry, and probing the new physics (NP) beyond the Standard Model (SM). Angular momentum conservation leads to three independent configurations of the vector mesons which reflects into three amplitudes. In the transversity basis, the decay amplitude can be decomposed into three independent components A_0 , A_{\parallel} , and A_{\perp} [1, 2], which correspond to longitudinal, parallel, and perpendicular polarizations of the final-state spin vectors, respectively. Experimentally they are at least four-body decays [3], since a vector resonance is usually detected via its decay $V \rightarrow PP'$ with $P^{(\prime)}$ being a pseudoscalar. As the vector meson has a relatively broad width, there is generally a background due to the (resonant or nonresonant) scalar production of the two pseudoscalars [4, 5] around the vector resonance region. In this case, it is necessary to add another three scalar amplitudes to the angular analysis in presence of the scalar background [6]. Then one can extract more CP -violating observables from the interference of the various helicity amplitudes. Therefore, the four-body charmless B decays through two vector intermediate states are rich in CP violating phenomena in the flavor sector involving quarks.

A four-body decay gives rise to three independent final momenta \vec{p}_i with $i = 1, 2, 3$ in the rest frame of the decaying parent particle, allows one to form a scalar triple product (TP) of $\vec{p}_1 \cdot (\vec{p}_2 \times \vec{p}_3)$. Obviously, it is odd under both parity and time reversal, and thus constitutes a potential signal of CP violation assuming CPT invariance. One can compare event distributions for positive TP against those with negative TP to construct a triple product asymmetry

*Corresponding author: liyakelly@163.com

†Corresponding author: jindui1127@126.com

(TPA),

$$A_T \equiv \frac{\Gamma(TP > 0) - \Gamma(TP < 0)}{\Gamma(TP > 0) + \Gamma(TP < 0)}, \quad (1)$$

where Γ is the partial decay rate in the indicated TP range. However, since both the final-state interaction and CP violation can produce the nonzero TPAs, one has to compare this asymmetry with a corresponding quantity in the CP conjugate process to obtain the “true” CP violation signal. Furthermore, unlike the direct CP violation, a nonzero true TPA does not require the presence of a nonzero strong phase [7], whilst it is maximal when the strong phase difference vanishes. In this case, it could be more promising to search for TPA than direct CP asymmetries in B decays. Therefore, the TPA is one of powerful tool for displaying CP violation in weak four-body decays [8, 9]. Further information on this rich subject may be found in Refs. [6–14].

Four-body decays of B meson are more complicated than two-body case, specifically where both nonresonant and resonant contribution exist. In our previous works [15, 16], the PQCD factorization formalism based on the quasi-two-body decay mechanism [17–19] for four-body B meson decays have been well established. That is, a four-particle final state is obtained through two intermediate resonances. The resonances decaying into meson pair are modeled by nonperturbative two-hadron distribution amplitudes (DAs) [20–26], which collect both resonant and nonresonant contributions [27]. In this work the similar strategy is extended to the penguin-dominated four-body decays $B \rightarrow \phi(\rightarrow K\bar{K})K^*(\rightarrow K\pi)$, which exhibit particularly alluring experimental and theoretical features.

In the SM, the decay $B \rightarrow \phi K^*$ are described by a loop mediated $b \rightarrow d$ or $b \rightarrow s$ transitions, providing a sensitive test for NP. The $B^0 \rightarrow \phi K^*$ decay was first observed by the CLEO collaboration [28]. Subsequently, branching ratio measurements and angular analyses have been reported by the BABAR and Belle collaborations [29–36]. The branching ratio as averaged by the Particle Data Group (PDG) is $(1.00 \pm 0.05) \times 10^{-5}$ [37], in good agreement with theoretical predictions [38, 39]. The observed surprisingly large transverse polarization fractions, contrary to naive predictions based on helicity arguments (the so-called polarization puzzle [37]), attracts much theoretical attention, with several explanations proposed [40–57]. Including both the S -wave $K^+\pi^-$ and K^+K^- contributions, the LHCb collaboration measured the polarization amplitudes and CP asymmetries in $B^0 \rightarrow \phi(\rightarrow K^+K^-)K^{*0}(\rightarrow K^+\pi^-)$ decay [58]. The angular analysis was used to determine TPAs for the first time. The measured true asymmetries show no significant deviations from zero, while several significant fake TPAs are consistent with the presence of final-state interactions. As for the B_s counterpart, the first observation of the decay $B_s^0 \rightarrow \phi\bar{K}^{*0}$, with $\phi \rightarrow K^+K^-$ and $\bar{K}^{*0} \rightarrow K^-\pi^+$, was reported by the LHCb experiment [59], meanwhile, the determination of its branching ratio and polarizations were presented, and the S -wave contribution was estimated to be in the teens. The measured value of branching ratio is significantly larger than the theoretical predictions [38, 60–65].

As discussed above, we focus on the four-body decays $B \rightarrow \phi(\rightarrow K\bar{K})K^*(\rightarrow K\pi)$, where the invariant mass of the $K\bar{K}$ ($K\pi$) pair is restricted to be within ± 15 MeV (± 150 MeV) of the known mass of the $\phi(K^*(892))$ meson for comparison with the LHCb data. Except for the dominant vector resonances, two important scalar backgrounds, such as $f_0(980) \rightarrow K\bar{K}$ and $K_0^*(1430) \rightarrow K\pi$, are also taken into account. The contributions from higher spin resonances are expected to be small in the concerned mass regions and are thus neglected in the following analysis. Six different quasi-two-body decay channels are considered, corresponding to various different possible combinations of $K\bar{K}$ and $K\pi$ pairs with spin 0 and 1. The S and P -wave contributions are parametrized into the corresponding timelike form factors involved in the two meson DAs, which are well established in the three-body B decays [66, 67]. With these universal nonperturbative quantities, we can make quantitative predictions on the various observables including the branching ratios, S -wave fractions, polarization fractions, direct CP violations, and the TPAs in $B \rightarrow \phi(\rightarrow K\bar{K})K^*(\rightarrow K\pi)$ decays.

The rest of the paper is organized as follows. Sec. II includes a general description of the angular distribution, kinematics, and the two meson distribution amplitudes of the considered four-body decays. We then apply the PQCD formalism in Sec. III to the $B \rightarrow \phi(\rightarrow K\bar{K})K^*(\rightarrow K\pi)$ decays. The numerical results are discussed and compared with those of other works in the literature. Sec. IV contains our conclusions. The relevant factorization formulas are collected in appendix A.

II. KINEMATICS AND TWO-MESON DISTRIBUTION AMPLITUDES

A. Angular distribution and the helicity amplitudes

The angular distribution in the $B^0 \rightarrow \phi K^{*0}$ decay with $\phi \rightarrow K^+K^-$ and $K^{*0} \rightarrow K^+\pi^-$ is described by three angles θ_1 , θ_2 , and ϕ in the helicity basis, which are depicted in Fig. 1. θ_1 is the polar angle of the K^+ in the rest frame of the K^* with respect to the helicity axis. Similarly, θ_2 is the polar angle of the K^+ in the ϕ rest frame with respect

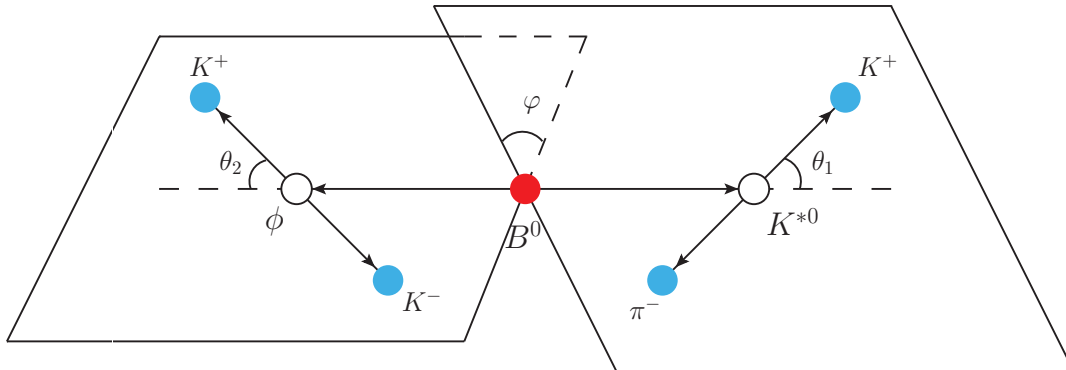


FIG. 1: The definition of the decay angles θ_1 , θ_2 , and φ for the decay $B^0 \rightarrow \phi K^{*0}$ with $\phi \rightarrow K^+ K^-$ and $K^{*0} \rightarrow K^+ \pi^-$. The angles are described in the text.

TABLE I: Quasi-two-body decay channels and the corresponding helicity amplitudes contributing to the $(K\bar{K})(K\pi)$ final state. The subscript S/P denotes a S - or P -wave configuration of the meson pair.

Quasi-two-body modes	Resonance types	Allowed helicity amplitudes
$B \rightarrow (K\bar{K})_P(K\pi)_P$	vector-vector	$A_{0,\parallel,\perp}$
$B \rightarrow (K\bar{K})_S(K\pi)_P$	scalar-vector	A_{SV}
$B \rightarrow (K\bar{K})_P(K\pi)_S$	vector-scalar	A_{VS}
$B \rightarrow (K\bar{K})_S(K\pi)_S$	scalar-scalar	A_{SS}

to the helicity axis of the ϕ . The azimuth angle φ is the relative angle between the $K^+ K^-$ and $K^+ \pi^-$ decay planes in the B rest frame.

Angular momentum conservation, for the vector-vector modes, allows three possible polarization configurations of the $K\bar{K}$ and $K\pi$ pairs, such as longitudinal, parallel, or perpendicular. The corresponding amplitudes are denoted by A_0 , A_{\parallel} , and A_{\perp} respectively, following the definitions given in Ref. [15]. Some scalar resonances, such as $f_0(980)$ and $K_0^*(1430)$, are expected to contribute and thus are included in the selected region of $K\bar{K}$ or $K\pi$ invariant masses. As one of the meson pair is produced in a spin-0 (S -wave) state, the resultant two single S -wave amplitudes are denoted as A_{SV} and A_{VS} , which are physical different. The double S -wave amplitude A_{SS} is associated with the final state, where both meson pairs are produced in the S wave. All of above considered decay modes, together with the corresponding amplitudes, are shown in Table I.

As discussed in Ref. [15], in the PQCD approach, these helicity amplitudes are expressed as the convolution of the hard kernels with the two-meson DAs, which absorb the nonperturbative dynamics involved in the meson pairs. After regularizing the end-point singularities and smearing the double logarithmic divergence, the typical factorization formula in coordinate space reads as

$$A \propto \int dx_B dx_1 dx_2 b_B db_B b_1 db_1 b_2 db_2 \text{Tr}[C(t)\Phi_B(x_B, b_B)\Phi_{K\pi}(x_1)\Phi_{K\bar{K}}(x_2)H(x_i, b_i, t)S_t(x_i)e^{-S(t)}], \quad (2)$$

where x_i and b_i with $i = B, 1, 2$ are the parton momentum fractions and the conjugate space coordinate of the transverse momentum, respectively. The threshold function $S_t(x_i)$ and the Sudakov exponents $S(t)$ are given in Appendix of Ref.[15]. t is the largest energy scale in hard function H . $C(t)$ is the short distance Wilson coefficients at the hard scale t . “Tr” denotes the trace over all Dirac structure and color indices. The explicit analytic formulas for the considered helicity amplitudes are presented in the appendix.

B. The kinematics of four-body decay

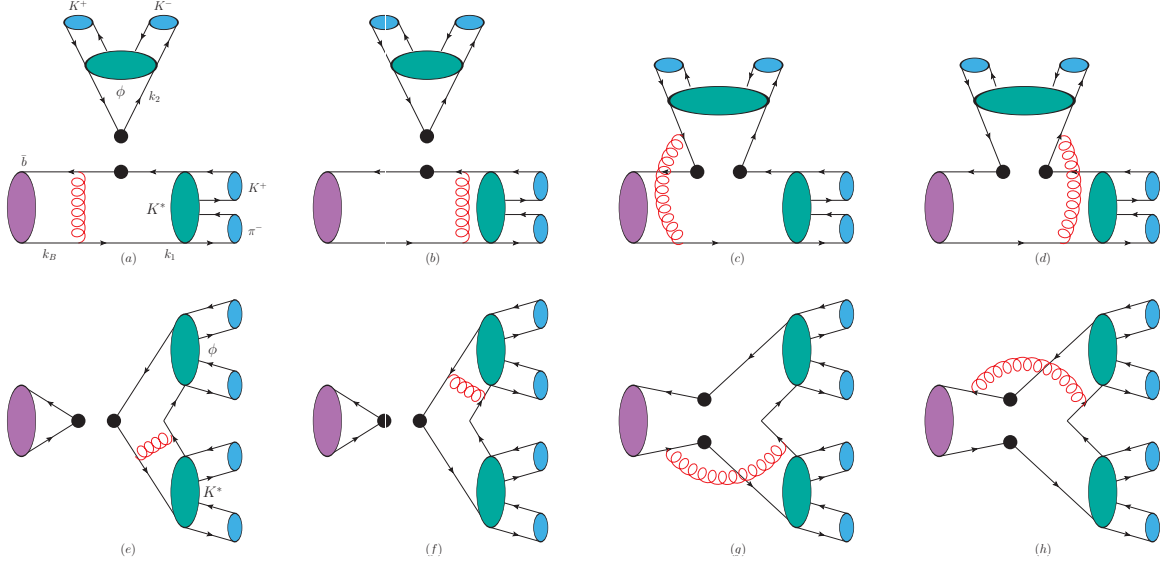


FIG. 2: Leading-order diagrams for the $B \rightarrow \phi(\rightarrow K\bar{K})K^*(\rightarrow K\pi)$ decays, where the symbol \bullet denotes a weak vertex.

Taking the full cascade decay $B \rightarrow \phi(\rightarrow K\bar{K})K^*(\rightarrow K\pi)$ as an example, the kinematics can be described in term of five independent variables: three helicity angles ($\theta_1, \theta_2, \varphi$) and two invariant masses ($m_{KK}, m_{K\pi}$). We first consider the subprocess $B \rightarrow \phi K^*$, where ϕ and K^* go subsequently into $K\bar{K}$ and $K\pi$ pairs, respectively. Following the definition given in Ref. [15], the external momenta of the decay chain will be denoted as p, q for the two meson pairs, and $p_{1,2}^{(\prime)}$ for the four final state mesons, with the specific charge assignment according to

$$B(p_B) \rightarrow \phi(q)K^*(p) \rightarrow K(p_2)\bar{K}(p'_2)K(p_1)\pi(p'_1), \quad (3)$$

where $p_B = p + q$, $p = p_1 + p'_1$, and $q = p_2 + p'_2$, which obey the momentum conservation. For simplicity, we shall work in the rest frame of the B meson in the light-cone coordinates such that $p_B = \frac{M}{\sqrt{2}}(1, 1, \mathbf{0}_T)$ with the B meson mass M . The momenta of ϕ and K^* can be written as

$$q = \frac{M}{\sqrt{2}}(f^-, f^+, \mathbf{0}_T), \quad p = \frac{M}{\sqrt{2}}(g^+, g^-, \mathbf{0}_T), \quad (4)$$

respectively. The factors g^\pm and f^\pm are related to the invariant masses of the meson pairs via $p^2 = \omega_1^2$ and $q^2 = \omega_2^2$, which can be written as

$$\begin{aligned} g^\pm &= \frac{1}{2}[1 + \eta_1 - \eta_2 \pm \sqrt{(1 + \eta_1 - \eta_2)^2 - 4\eta_1}], \\ f^\pm &= \frac{1}{2}[1 - \eta_1 + \eta_2 \pm \sqrt{(1 + \eta_1 - \eta_2)^2 - 4\eta_1}], \end{aligned} \quad (5)$$

with the mass ratios $\eta_{1,2} = \omega_{1,2}^2/M^2$. For the meson pairs in the P -wave configurations, the corresponding longitudinal polarization vectors are defined as

$$\epsilon_q = \frac{1}{\sqrt{2}\eta_2}(-f^-, f^+, \mathbf{0}_T), \quad \epsilon_p = \frac{1}{\sqrt{2}\eta_1}(g^+, -g^-, \mathbf{0}_T), \quad (6)$$

which satisfy the normalization $\epsilon_q^2 = \epsilon_p^2 = -1$ and the orthogonality $\epsilon_q \cdot q = \epsilon_p \cdot p = 0$.

Introducing the meson momentum fraction ζ for each meson pair, the individual momenta of the four final states can be expressed as

$$\begin{aligned}
p_1 &= \left(\frac{M}{\sqrt{2}} \left(\zeta_1 + \frac{r_1 - r'_1}{2\eta_1} \right) g^+, \frac{M}{\sqrt{2}} \left(1 - \zeta_1 + \frac{r_1 - r'_1}{2\eta_1} \right) g^-, \mathbf{p}_T \right), \\
p'_1 &= \left(\frac{M}{\sqrt{2}} \left(1 - \zeta_1 - \frac{r_1 - r'_1}{2\eta_1} \right) g^+, \frac{M}{\sqrt{2}} \left(\zeta_1 - \frac{r_1 - r'_1}{2\eta_1} \right) g^-, -\mathbf{p}_T \right), \\
p_2 &= \left(\frac{M}{\sqrt{2}} \left(1 - \zeta_2 + \frac{r_2 - r'_2}{2\eta_2} \right) f^-, \frac{M}{\sqrt{2}} \left(\zeta_2 + \frac{r_2 - r'_2}{2\eta_2} \right) f^+, \mathbf{q}_T \right), \\
p'_2 &= \left(\frac{M}{\sqrt{2}} \left(\zeta_2 - \frac{r_2 - r'_2}{2\eta_2} \right) f^-, \frac{M}{\sqrt{2}} \left(1 - \zeta_2 - \frac{r_2 - r'_2}{2\eta_2} \right) f^+, -\mathbf{q}_T \right),
\end{aligned} \tag{7}$$

with the mass ratios $r_i^{(\prime)} = m_i^{(\prime)2}/M^2$ ($i = 1, 2$), $m_i^{(\prime)}$ being the mass of the meson $P_i^{(\prime)}$. The transverse momenta \mathbf{p}_T and \mathbf{q}_T can be derived from the on-shell condition $p_i^{(\prime)2} = m_i^{(\prime)2}$ for each final-state meson, which yields

$$|\mathbf{p}_T|^2 = \omega_1^2 [\zeta_1(1 - \zeta_1) + \alpha_1], \quad |\mathbf{q}_T|^2 = \omega_2^2 [\zeta_2(1 - \zeta_2) + \alpha_2], \tag{8}$$

with the factors

$$\alpha_i = \frac{(r_i - r'_i)^2}{4\eta_i^2} - \frac{r_i + r'_i}{2\eta_i}. \tag{9}$$

Comparing Eqs. (4) and (7), we find the meson momentum fractions modified by the meson masses,

$$\frac{p_1^+}{p^+} = \zeta_1 + \frac{r_1 - r'_1}{2\eta_1}, \quad \frac{p_2^-}{q^-} = \zeta_2 + \frac{r_2 - r'_2}{2\eta_2}. \tag{10}$$

It is easy to derive the relation between ζ and the polar angles θ in Fig. 1 in the meson-pair rest frame:

$$2\zeta_i - 1 = \sqrt{1 + 4\alpha_i} \cos\theta_i, \tag{11}$$

with the bound

$$\zeta_i \in \left[\frac{1 - \sqrt{1 + 4\alpha_i}}{2}, \frac{1 + \sqrt{1 + 4\alpha_i}}{2} \right]. \tag{12}$$

Note that Eq. (11) reduces to the conventional form in Refs. [68, 69] in the limit of massless.

The Feynman diagrams for the hard kernels associated with the considered four-body B meson decays are displayed in Fig. 2, each of which contains a single hard gluon exchange at leading order in the PQCD approach. The first row represents the emission type, while the second row represents the annihilation one. Each type are further classified as factorizable, in which a gluon attaches to quarks in the same meson, and nonfactorizable, in which a gluon attaches to quarks in distinct mesons. For the evaluation of the hard kernels, we define three valence quark momenta labelled by k_B , k_1 , and k_2 in Fig. 2(a) as

$$k_B = (0, x_B p_B^-, \mathbf{k}_{BT}), \quad k_1 = (x_1 p^+, 0, \mathbf{k}_{1T}), \quad k_2 = (0, x_2 q^-, \mathbf{k}_{2T}), \tag{13}$$

with the parton momentum fractions x_i , and the parton transverse momenta k_{iT} . Since k_1 and k_2 move with the corresponding meson pair in the plus and minus direction, respectively. The minus (plus) component of k_1 (k_2) can be neglected due to its small size. We also drop k_B^+ because it does not appear in the hard kernels for dominant factorizable contributions.

C. Two-meson distribution amplitudes

The light-cone matrix elements for S -wave $K\bar{K}$ and $K\pi$ can be decomposed, up to the twist 3, into [17, 27]

$$\begin{aligned}
\Phi_{(K\bar{K})_S}(x_2, \omega_2) &= \frac{1}{\sqrt{2N_c}} [\not{q} \phi_{(K\bar{K})_S}^0(x_2, \omega_2) + \omega_2 \phi_{(K\bar{K})_S}^s(x_2, \omega_2) + \omega_2 (\not{p}\not{q} - 1) \phi_{(K\bar{K})_S}^t(x_2, \omega_2)], \\
\Phi_{(K\pi)_S}(x_1, \omega_1) &= \frac{1}{\sqrt{2N_c}} [\not{p} \phi_{(K\pi)_S}^0(x_1, \omega_1) + \omega_1 \phi_{(K\pi)_S}^s(x_1, \omega_1) + \omega_1 (\not{p}\not{q} - 1) \phi_{(K\pi)_S}^t(x_1, \omega_1)],
\end{aligned} \tag{14}$$

with $n = (1, 0, \mathbf{0}_T)$ and $v = (0, 1, \mathbf{0}_T)$ being two dimensionless vectors. The parameterization of various twists DAs take the forms

$$\begin{aligned}\phi_{(PP')_S}^0(x, \omega) &= \begin{cases} \frac{9F_{(PP')_S}(\omega)}{\sqrt{2N_c}} a_{PP'} x(1-x)(1-2x), & PP' = K\bar{K}, \\ \frac{3F_{(PP')_S}(\omega)}{\sqrt{2N_c}} x(1-x) \left[\frac{1}{\mu_S} + B_1 3(1-2x) + B_3 \frac{5}{2}(1-2x)(7(1-2x)^2 - 3) \right], & PP' = K\pi, \end{cases} \\ \phi_{(PP')_S}^s(x, \omega) &= \frac{F_{(PP')_S}(\omega)}{2\sqrt{2N_c}}, \\ \phi_{(PP')_S}^t(x, \omega) &= \frac{F_{(PP')_S}(\omega)}{2\sqrt{2N_c}}(1-2x),\end{aligned}\quad (15)$$

with the ratio $\mu_S = \omega_1/(m_s - m_q)$, where $m_s(1 \text{ GeV}) = 119 \text{ MeV}$ [70, 71] is the running strange quark mass and the light quark masses m_q , $q = u, d$, are set to zero. The values of the Gegenbauer moments for the twist-2 DAs are taken as [66, 70–72]

$$a_{K\bar{K}} = 0.80 \pm 0.16, \quad B_1 = -0.57 \pm 0.13, \quad B_3 = -0.42 \pm 0.22. \quad (16)$$

Because the available data are not yet precise enough to extract more Gegenbauer moments, the two twist-3 DAs are chosen as asymptotic forms.

For the scalar form factor $F_{(K\pi)_S}$, we follow the LASS line shape [73], which includes an effective-range nonresonant component with the $K_0^*(1430)$ resonance Breit-Wigner tail. The explicit expression is given by

$$\begin{aligned}F_{(K\pi)_S}(\omega) &= \frac{\omega}{k(\omega)} \cdot \frac{1}{\cot \delta_B - i} + e^{2i\delta_B} \frac{m_0^2 \Gamma_0 / k(m_0)}{m_0^2 - \omega^2 - im_0^2 \frac{\Gamma_0}{\omega} \frac{k(\omega)}{k(m_0)}}, \\ \cot \delta_B &= \frac{1}{ak(\omega)} + \frac{1}{2}bk(\omega),\end{aligned}\quad (17)$$

where m_0 (Γ_0) is the mass (width) of $K_0^*(1430)$. The kaon three-momentum $k(\omega)$ is written, in the $K\pi$ center-of-mass frame, as

$$k(\omega) = \frac{\sqrt{[\omega^2 - (m_K + m_\pi)^2][\omega^2 - (m_K - m_\pi)^2]}}{2\omega}, \quad (18)$$

with $m_{K(\pi)}$ the known kaon (pion) mass, and $k(m_0)$ being the same quantity evaluated at the nominal resonance mass m_0 . We use the following values for the resonance mass, width, scattering length and effective-range parameters: $m_0 = 1450 \pm 80 \text{ MeV}$, $\Gamma_0 = 400 \pm 230 \text{ MeV}$, $a = 3.2 \pm 1.8 \text{ GeV}^{-1}$ and $b = 0.9 \pm 1.1 \text{ GeV}^{-1}$ [15, 74].

For the scalar form factor of the $K\bar{K}$ system, the main resonance is $f_0(980)$ in the concerned mass window. Since its mass is very close to the $K\bar{K}$ threshold, which can strongly influence the resonance shape. We follow Ref. [66] to take the the widely accepted prescription proposed by Flatté [75]

$$F_{(K\bar{K})_S}(\omega) = \frac{m_{f_0(980)}^2}{m_{f_0(980)}^2 - \omega^2 - im_{f_0(980)}(g_{\pi\pi}\rho_{\pi\pi} + g_{KK}\rho_{KK}F_{KK}^2)} \quad (19)$$

with $m_{f_0(980)} = 939 \text{ MeV}/c^2$, $g_{\pi\pi} = 199 \text{ MeV}/c^2$, $g_{KK} = 3g_{\pi\pi}$ [58]. The exponential term $F_{KK} = e^{-\alpha q_k^2}$ is introduced above the $K\bar{K}$ threshold to reduce the ρ_{KK} factor as ω increases, where q_k is the momentum of the kaon in the $K\bar{K}$ rest frame and $\alpha = 2.0 \pm 0.25 \text{ GeV}^{-2}$ [76, 77].

In Ref. [15] we have updated the P -wave DAs including both longitudinal and transverse polarizations for the $K\pi$ pair, whose explicit expressions read

$$\begin{aligned}\Phi_{(K\pi)_P}^L(x_1, \zeta_1, \omega_1) &= \frac{1}{\sqrt{2N_c}} [\omega_1 \not{\epsilon}_P \phi_{(K\pi)_P}^0(x_1, \omega_1) + \omega_1 \phi_{(K\pi)_P}^s(x_1, \omega_1) + \frac{\not{\psi}_1 \not{\psi}'_1 - \not{\psi}'_1 \not{\psi}_1}{\omega_1(2\zeta_1 - 1)} \phi_{(K\pi)_P}^t(x_1, \omega_1)] (2\zeta_1 - 1), \\ \Phi_{(K\pi)_P}^T(x_1, \zeta_1, \omega_1) &= \frac{1}{\sqrt{2N_c}} [\gamma_5 \not{\epsilon}_T \not{\psi} \phi_{(K\pi)_P}^T(x_1, \omega_1) + \omega_1 \gamma_5 \not{\epsilon}_T \phi_{(K\pi)_P}^a(x_1, \omega_1) + i\omega_1 \frac{\epsilon^{\mu\nu\rho\sigma} \gamma_\mu \epsilon_{T\nu} p_\rho n_{-\sigma}}{p \cdot n_-} \phi_{(K\pi)_P}^v(x_1, \omega_1)] \\ &\quad \sqrt{\zeta_1(1 - \zeta_1) + \alpha_1},\end{aligned}\quad (20)$$

respectively. Naively, the P -wave $K\bar{K}$ ones can be obtained with the following replacement:

$$x_1 \rightarrow x_2, \omega_1 \rightarrow \omega_2, \zeta_1 \rightarrow \zeta_2, \alpha_1 \rightarrow \alpha_2, p \rightarrow q, \epsilon_p \rightarrow \epsilon_q, p_1^{(\prime)} \rightarrow p_2^{(\prime)}. \quad (21)$$

The various twist DAs for the P -wave $K\bar{K}$ and $K\pi$ systems are parametrized as [67]

$$\begin{aligned} \phi_{K\bar{K}}^0(x_2, \omega_2) &= \frac{3}{\sqrt{2N_c}} F_{K\bar{K}}^\parallel(\omega_2) x_2 (1-x_2) [1 + a_{2\phi}^0 C_2^{3/2}(2x_2 - 1)], \\ \phi_{K\bar{K}}^s(x_2, \omega_2) &= \frac{3}{2\sqrt{2N_c}} F_{K\bar{K}}^\perp(\omega_2) (1-2x_2), \\ \phi_{K\bar{K}}^t(x_2, \omega_2) &= \frac{3}{2\sqrt{2N_c}} F_{K\bar{K}}^\perp(\omega_2) (1-2x_2)^2, \\ \phi_{K\bar{K}}^T(x_2, \omega_2) &= \frac{3}{\sqrt{2N_c}} F_{K\bar{K}}^\perp(\omega_2) x_2 (1-x_2) [1 + a_{2\phi}^0 C_2^{3/2}(2x_2 - 1)], \\ \phi_{K\bar{K}}^a(x_2, \omega_2) &= \frac{3}{4\sqrt{2N_c}} F_{K\bar{K}}^\parallel(\omega_2) (1-2x_2), \\ \phi_{K\bar{K}}^v(x_2, \omega_2) &= \frac{3}{8\sqrt{2N_c}} F_{K\bar{K}}^\parallel(\omega_2) [1 + (1-2x_2)^2], \\ \phi_{K\pi}^0(x_1, \omega_1) &= \frac{3}{\sqrt{2N_c}} F_{K\pi}^\parallel(\omega_1) x_1 (1-x_1) [1 + a_{1K^*}^0 C_1^{3/2}(2x_1 - 1) + a_{2K^*}^0 C_2^{3/2}(2x_1 - 1)], \\ \phi_{K\pi}^s(x_1, \omega_1) &= \frac{3}{2\sqrt{2N_c}} F_{K\pi}^\perp(\omega_1) (1-2x_1), \\ \phi_{K\pi}^t(x_1, \omega_1) &= \frac{3}{2\sqrt{2N_c}} F_{K\pi}^\perp(\omega_1) (1-2x_1)^2, \\ \phi_{K\pi}^T(x_1, \omega_1) &= \frac{3}{\sqrt{2N_c}} F_{K\pi}^\perp(\omega_1) x_1 (1-x_1) [1 + a_{1K^*}^0 C_1^{3/2}(2x_1 - 1) + a_{2K^*}^0 C_2^{3/2}(2x_1 - 1)], \\ \phi_{K\pi}^a(x_1, \omega_1) &= \frac{3}{4\sqrt{2N_c}} F_{K\pi}^\parallel(\omega_1) (1-2x_1), \\ \phi_{K\pi}^v(x_1, \omega_1) &= \frac{3}{8\sqrt{2N_c}} F_{K\pi}^\parallel(\omega_1) [1 + (1-2x_1)^2], \end{aligned} \quad (22)$$

with the Gegenbauer polynomials

$$C_1^{3/2}(t) = 3t, \quad C_2^{3/2}(t) = \frac{3}{2}(5t^2 - 1). \quad (23)$$

The values of the Gegenbauer moments associated with longitudinal polarization are adopted as

$$a_{1K^*}^0 = 0.31 \pm 0.16, \quad a_{2K^*}^0 = 1.19 \pm 0.10, \quad a_{2\phi}^0 = -0.31 \pm 0.19, \quad (24)$$

which are determined from a global analysis in the PQCD approach [67]. We do not distinguish the Gegenbauer moments for the longitudinal and transverse polarizations in our numerical calculations due to a lack of rigorous theoretical and experimental information on the transverse polarizations.

Since the $K\pi$ spectrum is dominated by the vector $K^*(892)$ resonance in the selected invariant mass range, the P -wave time-like form factor $F_{K\pi}^\parallel$ is parametrized as the relativistic Breit-Wigner (RBW) model [78, 79]

$$F_{K\pi}^\parallel(\omega) = \frac{m_{K^*}^2}{m_{K^*}^2 - \omega^2 - im_{K^*}\Gamma(\omega)}, \quad (25)$$

where $m_{K^*} = 895.81$ MeV is the $K^*(892)$ mass. The mass-dependent width is given by

$$\Gamma(\omega) = \Gamma_{K^*} \frac{k^3(\omega)}{k^3(m_{K^*})} \frac{m_{K^*}}{\omega} \frac{1 + r^2 k^2(m_{K^*})}{1 + r^2 k^2(\omega)}, \quad (26)$$

where $\Gamma_{K^*} = 47.4$ MeV is the natural width of the $K^*(892)$ meson and $r = 3.4$ GeV⁻¹ is the interaction radius [58]. For the P -wave $K\bar{K}$ one, denoted $F_{K\bar{K}}^\parallel$, is modelled in a similar way using the values $m_\phi = 1019.455$ MeV and $\Gamma_\phi = 4.26$ MeV [58]. For another form factor F^\perp , we assume the approximate relation $F^\perp/F^\parallel \sim f_V^T/f_V$ with $f_V^{(T)}$ being the tensor (vector) decay constant of the vector resonance.

TABLE II: The decay constants are taken from Refs. [15, 60, 67]. Other parameters are from PDG 2020 [37].

Mass(GeV)	$M_{B_s} = 5.37$		$M_B = 5.28$	$m_K = 0.494$	$m_\pi = 0.14$
Wolfenstein parameters	$\lambda = 0.22650$		$A = 0.790$	$\bar{\rho} = 0.141$	$\bar{\eta} = 0.357$
Decay constants (GeV)	$f_{B_s} = 0.24$	$f_B = 0.21$	$f_{\phi(1020)} = 0.215$	$f_{\phi(1020)}^T = 0.186$	$f_{K^*} = 0.217$ $f_{K^*}^T = 0.185$
Lifetime (ps)	$\tau_{B_s} = 1.51$		$\tau_{B^0} = 1.52$		$\tau_{B^+} = 1.638$

III. NUMERICAL RESULTS

In this section we discuss in detail some physical observables, such as branching ratios, S -wave fractions, polarization fractions, direct CP asymmetries, and TPAs, for the concerned decays. The related input parameters for the numerical calculations are collected in Table II. The decay constants are used the values from Refs. [15, 60, 67], while the meson masses, Wolfenstein parameters, and the lifetimes are taken from the PDG review [37]. We neglect uncertainties on the constants since they are negligible with respect to other sources of uncertainty. The parameters relevant to the $K\bar{K}$ and $K\pi$ DAs have been specified in the previous section.

Another key input in the PQCD calculations is the B meson distribution amplitude. We adopt the conventional form from Refs. [80, 81] of the leading Lorentz structure

$$\phi_B(x, b) = N_B x^2 (1-x)^2 \exp\left[-\frac{x^2 M^2}{2\omega_b^2} - \frac{\omega_b^2 b^2}{2}\right], \quad (27)$$

with the shape parameter $\omega_b = 0.40$ GeV for $B_{u,d}$ mesons and $\omega_b = 0.48$ GeV for a B_s meson [82]. The normalization constant N_B being related to the decay constant f_B via the normalization

$$\int_0^1 \phi_B(x, b=0) dx = \frac{f_B}{2\sqrt{2}N_c}. \quad (28)$$

For more alternative models of B meson DA and the subleading contributions, one can refer to Refs. [83–87].

A. CP averaged four-body branching ratios and S -wave fractions

The phase space of a four-body decay relies on the five kinematic variables, that is, three helicity angles shown in Fig. 1 and two invariant masses. In the B meson rest frame, the five-fold differential decay rate can be written as

$$\frac{d^5\Gamma}{d\theta_1 d\theta_2 d\varphi d\omega_1 d\omega_2} = \frac{k(\omega_1)k(\omega_2)k(\omega_1, \omega_2)}{16(2\pi)^6 M^2} |A|^2, \quad (29)$$

where $k(\omega_1, \omega_2) = \sqrt{[M^2 - (\omega_1 + \omega_2)^2][M^2 - (\omega_1 - \omega_2)^2]}/(2M)$ is the magnitude of the three-momentum of the meson pair in the B meson rest frame. By appropriate variable changes, Eq. (29) is equivalent to the one in Ref. [88]. Replacing the helicity angles θ_i by the meson momentum fractions ζ_i via Eq. (11) and integrating the decay rate with respect to all independent variables, we obtain

$$\Gamma = \frac{1}{4(2\pi)^6 M^2 \sqrt{1+4\alpha_1} \sqrt{1+4\alpha_2}} \int k(\omega_1)k(\omega_2)k(\omega_1, \omega_2) |A|^2 d\zeta_1 d\zeta_2 d\varphi d\omega_1 d\omega_2, \quad (30)$$

where the selected invariant mass ranges for the $K\bar{K}$ and $K\pi$ pairs are $m_\phi - 0.015 < \omega_2 < m_\phi + 0.015$ (GeV) and $m_{K^*} - 0.15 < \omega_1 < m_{K^*} + 0.15$ (GeV), respectively. The total amplitude (A) can be decomposed into six helicity components shown in Table I with different ζ_i and φ dependencies [15]

$$\begin{aligned} A = & \frac{2\zeta_1 - 1}{\sqrt{1+4\alpha_1}} \frac{2\zeta_2 - 1}{\sqrt{1+4\alpha_2}} A_0 + 2\sqrt{2} \sqrt{\frac{\zeta_1(1-\zeta_1) + \alpha_1}{1+4\alpha_1}} \sqrt{\frac{\zeta_2(1-\zeta_2) + \alpha_2}{1+4\alpha_2}} \cos(\varphi) A_{\parallel} \\ & + i2\sqrt{2} \sqrt{\frac{\zeta_1(1-\zeta_1) + \alpha_1}{1+4\alpha_1}} \sqrt{\frac{\zeta_2(1-\zeta_2) + \alpha_2}{1+4\alpha_2}} \sin(\varphi) A_{\perp} + \frac{2\zeta_1 - 1}{\sqrt{1+4\alpha_1}} A_{VS} \\ & + \frac{2\zeta_2 - 1}{\sqrt{1+4\alpha_2}} A_{SV} + A_{SS}. \end{aligned} \quad (31)$$

The branching ratio of each component is then

$$\mathcal{B}_h = \frac{\tau_B}{4(2\pi)^6 M^2} \frac{2\pi}{9} Y_h \int d\omega_1 d\omega_2 k(\omega_1) k(\omega_2) k(\omega_1, \omega_2) |A_h|^2, \quad (32)$$

with

$$Y_h = \begin{cases} 1, & h = 0, \parallel, \perp \\ 3, & h = SV, VS \\ 9, & h = SS. \end{cases} \quad (33)$$

which come from the integrations over $\zeta_1, \zeta_2, \varphi$. Combining Eq. (32) with its counterpart of the corresponding CP -conjugated process, we can derive the CP -averaged branching ratio of each component and their sum

$$\mathcal{B}_h^{avg} = \frac{1}{2} (\bar{\mathcal{B}}_h + \mathcal{B}_h), \quad \mathcal{B}_{\text{total}} = \sum_h \mathcal{B}_h, \quad (34)$$

with h running over the six helicities as stated above.

The numerical results are summarized in Table III, where the first quoted uncertainty is due to the shape parameters ω_b in the $B_{(s)}$ meson DAs with 10% variation, the second uncertainty is caused by the variation of the Gegenbauer moments in the two meson DAs shown in Eqs (16) and (24), and the last one come from the hard scale t that vary from $0.75t$ to $1.25t$ and the QCD scale $\Lambda_{QCD} = 0.25 \pm 0.05$ GeV. The three uncertainties are comparable, and their combined impacts could exceed 50%, implying that the nonperturbative parameters in the DAs of the initial and final states must be more precisely restricted, and the higher-order correction to four-body B meson decays is critical. The concerned three channels are all penguin-dominated decays. The B^0 and B^+ modes involve the $b \rightarrow s$ transition and therefore have relatively large branching ratios of $\mathcal{O}(10^{-7} \sim 10^{-6})$, while the B_s channels, mediated by the $b \rightarrow d$ transition, are generally one or two order of magnitudes smaller.

TABLE III: PQCD predictions for the CP -averaged branching ratios of various components and their sum in the $B_{(s)} \rightarrow (K\bar{K})(K\pi)$ decays within the $K\bar{K}(K\pi)$ invariant mass window of 15 (150) MeV around the $\phi(K^*(982))$ resonance.

Components	$B^0 \rightarrow (K^+K^-)(K^+\pi^-)$	$B_s^0 \rightarrow (K^+K^-)(K^-\pi^+)$	$B^+ \rightarrow (K^+K^-)(K^0\pi^+)$
\mathcal{B}_0	$1.8^{+0.7+0.3+0.6}_{-0.6-0.4-0.4} \times 10^{-6}$	$3.1^{+1.2+1.0+1.6}_{-0.8-0.9-1.2} \times 10^{-8}$	$1.8^{+0.9+0.4+0.7}_{-0.5-0.3-0.4} \times 10^{-6}$
\mathcal{B}_{\parallel}	$3.1^{+0.5+0.4+1.3}_{-0.4-0.4-0.8} \times 10^{-7}$	$5.3^{+0.6+2.0+2.5}_{-0.3-1.4-1.3} \times 10^{-9}$	$3.4^{+0.6+0.5+1.3}_{-0.4-0.4-0.8} \times 10^{-7}$
\mathcal{B}_{\perp}	$3.3^{+0.6+0.5+1.3}_{-0.4-0.4-0.8} \times 10^{-7}$	$5.2^{+0.3+1.9+2.6}_{-0.3-1.6-1.5} \times 10^{-9}$	$3.6^{+0.6+0.4+1.3}_{-0.5-0.5-0.9} \times 10^{-7}$
\mathcal{B}_{SS}	$4.7^{+2.0+2.4+1.8}_{-1.4-1.9-1.4} \times 10^{-8}$	$1.3^{+0.7+0.6+0.5}_{-0.5-0.5-0.4} \times 10^{-9}$	$5.2^{+2.1+2.6+2.0}_{-1.5-2.1-1.6} \times 10^{-8}$
\mathcal{B}_{VS}	$4.6^{+1.2+1.0+1.7}_{-0.9-1.0-1.4} \times 10^{-7}$	$5.0^{+2.3+1.2+2.7}_{-1.8-1.1-2.1} \times 10^{-9}$	$4.8^{+1.5+1.0+1.8}_{-1.1-1.0-1.3} \times 10^{-7}$
\mathcal{B}_{SV}	$2.2^{+0.6+0.4+0.8}_{-0.5-0.4-0.6} \times 10^{-7}$	$1.6^{+0.5+0.8+0.5}_{-0.4-0.6-0.4} \times 10^{-9}$	$2.5^{+0.7+0.5+0.9}_{-0.5-0.4-0.7} \times 10^{-7}$
$\mathcal{B}_{\text{total}}$	$3.2^{+1.0+0.4+1.1}_{-0.9-0.5-0.8} \times 10^{-6}$	$4.9^{+1.6+1.4+2.4}_{-1.1-1.2-1.6} \times 10^{-8}$	$3.3^{+1.2+0.6+1.2}_{-0.8-0.5-0.8} \times 10^{-6}$

Although the P -wave contributions dominate in the selected mass regions, the S -wave contributions, which are strongly sensitive to the integrating ranges, can not be neglected. In order to compare the relative size of the S -wave contributions, one can define the S -wave fractions as

$$f_{\sigma} = \frac{\mathcal{B}_{\sigma}}{\mathcal{B}_{\text{total}}}, \quad (35)$$

with $\sigma = \{SS, SV, VS\}$, and the total S -wave fraction as $f_{S\text{-wave}} = f_{SS} + f_{SV} + f_{VS}$. Using the PQCD predictions as given in Table III, it is straightforward to obtain the numerical results of S -wave fractions in each channel as exhibited in Table IV.

The predicted two single S -wave fractions for the B^0 mode are well consistent with the data from Ref. [58]. In Ref. [58], it is assumed that the double S -wave component is negligible. In our calculations, as can be seen in Table IV, the double S -wave fractions of all the three modes are estimated to be less than 3% and can be safely ignored. Therefore the assumption in [58] is reasonable in the selected invariant mass ranges. However, we will discuss later that the S -wave contributions will be enhanced rapidly with increasing invariant mass ranges. The predicted total S -wave fraction for the B_s mode is in agreement with the LHCb data 0.16 ± 0.02 [59] obtained from the total ϕK^{*0} purity by combining the K^+K^- and $K^+\pi^-$ contributions. It is assumed in Ref. [59] that the S -wave

component is the same for $B^0 \rightarrow \phi K^{*0}$ and $B_s^0 \rightarrow \phi \bar{K}^{*0}$ decays, so that the larger sample of $B^0 \rightarrow \phi K^{*0}$ decays can be used. This assumption lead to a large systematic uncertainty of this measurement, which is expected to scale with larger data samples in future. From Table IV, the total S -wave contributions could be as large as 20% of the total decay rate, indicate they are numerically significant in the given mass regions.

TABLE IV: S -wave fractions in the $B_{(s)} \rightarrow (K\bar{K})(K\pi)$ decays within the $K\bar{K}(K\pi)$ invariant mass window of 15 (150) MeV around the $\phi(K^*(982))$ resonance. The data are taken from Ref. [58], where the first uncertainty is statistical and the second is systematic.

Modes	f_{SS}	f_{VS}	f_{SV}	f_{S-wave}
$B^0 \rightarrow (K^+K^-)(K^+\pi^-)$	$0.015^{+0.001+0.007+0.002}_{-0.000-0.006-0.002}$	$0.144^{+0.013+0.022+0.016}_{-0.007-0.020-0.015}$	$0.069^{+0.006+0.014+0.002}_{-0.002-0.011-0.005}$	$0.228^{+0.020+0.037+0.018}_{-0.009-0.032-0.022}$
LHCb [58]	...	$0.143 \pm 0.013 \pm 0.012$	$0.122 \pm 0.013 \pm 0.008$...
$B_s^0 \rightarrow (K^+K^-)(K^-\pi^+)$	$0.027^{+0.004+0.013+0.002}_{-0.004-0.011-0.002}$	$0.102^{+0.010+0.032+0.022}_{-0.018-0.030-0.029}$	$0.033^{+0.000+0.016+0.004}_{-0.001-0.014-0.007}$	$0.162^{+0.014+0.057+0.027}_{-0.023-0.050-0.037}$
$B^+ \rightarrow (K^+K^-)(K^0\pi^+)$	$0.016^{+0.000+0.008+0.001}_{-0.001-0.006-0.002}$	$0.146^{+0.003+0.021+0.014}_{-0.006-0.021-0.009}$	$0.076^{+0.003+0.014+0.001}_{-0.005-0.013-0.007}$	$0.238^{+0.006+0.035+0.015}_{-0.012-0.035-0.018}$

The S -wave channels were also measured by other collaborations with different $K\pi$ mass range. The branching ratio for $B^0 \rightarrow \phi(K\pi)_0^*$ mode was measured to be $(4.3 \pm 0.4(\text{stat}) \pm 0.4(\text{syst})) \times 10^{-6}$ by the Belle experiment [35], which was consistent with previous BABAR measurement, $(4.3 \pm 0.6(\text{stat}) \pm 0.4(\text{syst})) \times 10^{-6}$ [32]. We note that above two measurements were performed in a broad $K\pi$ invariant mass range $0.7 < m_{K\pi} < 1.55$ GeV. For comparison, we derive the single S -wave branching ratio with the same mass region,

$$\mathcal{B}(B^0 \rightarrow \phi(\rightarrow K^+K^-)(K\pi)_0^*(\rightarrow K^+\pi^-)) = (1.2^{+0.4+0.3+0.5}_{-0.1-0.2-0.3}) \times 10^{-6}, \quad (36)$$

which is more than twice the number in Table III. After correcting for the secondary branching fraction $\mathcal{B}(\phi \rightarrow K^+K^-) = 0.5$ and $\mathcal{B}((K\pi)_0^* \rightarrow K^+\pi^-) = 2/3$, one can obtain the two-body decay branching ratio in the narrow-width limit,

$$\mathcal{B}(B^0 \rightarrow \phi(K\pi)_0^*) = (3.6^{+1.2+0.9+1.5}_{-0.3-0.6-0.9}) \times 10^{-6}, \quad (37)$$

comply with the above two measurements and the previous two-body PQCD value of $(3.7^{+0.8+0.1+3.7}_{-0.7-0.1-1.7}) \times 10^{-6}$ for the S1 scenario [89].

In Ref. [90], the BABAR collaboration measured the $B^0 \rightarrow f_0(980)K^{*0}(892)$ and $B^0 \rightarrow f_0(980)(K\pi)_0^*$ decays, where $f_0(980)$ was reconstructed through $f_0(980) \rightarrow \pi\pi$ within the $\pi\pi$ invariant mass range $0.47 < m_{\pi\pi} < 1.07$ GeV. For the $K\pi$ mass spectrum, the two channels were analyzed separately. The former was performed in the ‘‘low mass region’’ (LMR), $0.75 < m_{K\pi} < 1.0$ GeV, while the latter was performed in the ‘‘high mass region’’ (HMR), $1.0 < m_{K\pi} < 1.55$ GeV. The quoted branching ratios yield [90]

$$\begin{aligned} \mathcal{B}(B^0 \rightarrow f_0(980)(K\pi)_0^*) \times \mathcal{B}(f_0(980) \rightarrow \pi\pi) \times \mathcal{B}((K\pi)_0^* \rightarrow K\pi) &= (3.1 \pm 0.8 \pm 0.7) \times 10^{-6}, \\ \mathcal{B}(B^0 \rightarrow f_0(980)K^{*0}(892)) \times \mathcal{B}(f_0(980) \rightarrow \pi\pi) &= (5.7 \pm 0.6 \pm 0.4) \times 10^{-6}, \end{aligned} \quad (38)$$

where the uncertainties are statistical and systematic, respectively. Belle collaboration presented a smaller value of $\mathcal{B}(B^0 \rightarrow f_0(980)K^{*0}(892)) = (1.4^{+0.6+0.6}_{-0.5-0.4}) \times 10^{-6}$, obtained for $m_{K\pi} \in (0.75, 1.2)$ GeV and $m_{\pi\pi} \in (0.55, 1.2)$ GeV, with 2.5σ significance [91]. For comparison we recalculate the four-body branching ratios for the scalar-scalar and scalar-vector modes with the same $K\pi$ mass region as the BABAR experiment. In the narrow-width limit, we obtain the products

$$\begin{aligned} \mathcal{B}(B^0 \rightarrow f_0(980)(K\pi)_0^*) \times \mathcal{B}(f_0(980) \rightarrow K^+K^-) \times \mathcal{B}((K\pi)_0^* \rightarrow K^+\pi^-) &= (2.1^{+0.7+0.9+0.9}_{-0.6-0.7-0.6}) \times 10^{-7}, \\ \mathcal{B}(B^0 \rightarrow f_0(980)K^{*0}(892)) \times \mathcal{B}(f_0(980) \rightarrow K^+K^-) \times \mathcal{B}(K^{*0}(892) \rightarrow K^+\pi^-) &= (4.3^{+1.3+0.7+1.6}_{-0.9-0.7-1.2}) \times 10^{-7}. \end{aligned} \quad (39)$$

It is worth emphasizing that the above results cannot be directly compared with the data in Eq. (38) due to the absence of reliable information about $\mathcal{B}(f_0(980) \rightarrow K^+K^-)$ and $\mathcal{B}(f_0(980) \rightarrow \pi^+\pi^-)$. Assuming that the $f_0(980)$ resonance only couple to the $K\bar{K}$ and $\pi\pi$ channels and using the BES measurement [92]

$$\frac{\Gamma(f_0(980) \rightarrow \pi\pi)}{\Gamma(f_0(980) \rightarrow \pi\pi) + \Gamma(f_0(980) \rightarrow K\bar{K})} = 0.75^{+0.11}_{-0.13}, \quad (40)$$

and isospin relations $\Gamma(f_0(980) \rightarrow \pi^+\pi^-)/\Gamma(f_0(980) \rightarrow \pi\pi) = 2/3$ and $\Gamma(f_0(980) \rightarrow K^+K^-)/\Gamma(f_0(980) \rightarrow K\bar{K}) = 1/2$, we obtain the ratio

$$\frac{\Gamma(f_0(980) \rightarrow \pi^+\pi^-)}{\Gamma(f_0(980) \rightarrow K^+K^-)} = 4.0^{+0.6}_{-0.7}. \quad (41)$$

Plugging Eq. (41) into Eq. (39), and using above isospin relations, we estimate the branching ratio products in Eq. (38) to be $(1.9_{-1.0}^{+1.4}) \times 10^{-6}$ and $(3.9_{-1.5}^{+2.0}) \times 10^{-6}$, respectively, where the errors are added in quadrature. It can be seen that our prediction for the former is consistent with the BABAR value within uncertainties, but with central values that are somewhat lower. The number of the latter is in between BABAR and Belle measurements within errors. As pointed out in Refs. [93, 94], the narrow width approximation should be corrected by including finite-width effects for the broad scalar intermediate states. The results of Eq. (39), extracted from the four-body branching ratios, may suffer from a large uncertainty due to the finite-width effects of the scalar resonance. Thus the above comparisons just be a rough estimate for a cross-checking. In addition, we have shown that the S -wave contributions depend on the range of the $K\bar{K}$ and $K\pi$ invariant masses. In this study, the $K\bar{K}$ invariant mass is limited in a narrow window of ± 15 MeV around the known ϕ mass, a broader integrated region would increase our results. It is expected that future experiments can directly reconstruct intermediate $f_0(980)$ resonance through $f_0(980) \rightarrow K^+K^-$ in the $B^0 \rightarrow (K^+K^-)(K^+\pi^-)$ decay.

B. Two-body branching ratios and polarization fractions

TABLE V: CP -averaged branching ratios and polarization fractions for the two-body $B \rightarrow \phi K^*$ decays. For comparison, we also list the results from PQCD [52, 60, 62], QCDF [38, 39, 61, 95], SCET [63], and FAT [64]. The world averages of experimental data are taken from PDG 2020 [37].

Modes	$\mathcal{B}(10^{-6})$	$f_0(\%)$	$f_\perp(\%)$
$B^0 \rightarrow \phi K^{*0}$	$7.4_{-2.1-1.2-1.8}^{+2.5+1.1+2.6}$	$74.1_{-5.8-3.0-1.2}^{+3.1+1.5+1.1}$	$13.3_{-1.6-0.8-0.5}^{+3.0+1.6+0.6}$
PQCD-I [52]	14.86	75.0	11.5
PQCD-II [62]	$9.8_{-3.8}^{+4.9}$	$56.5_{-5.9}^{+5.8}$	$21.3_{-2.9}^{+2.8}$
QCDF-I [38]	$9.3_{-0.5-6.5}^{+0.5+11.4}$	44_{-0-36}^{+0+59}	...
QCDF-II [39]	$9.5_{-1.2-5.9}^{+1.3+11.9}$	50_{-42}^{+50}	25_{-25}^{+21}
SCET [63]	9.14 ± 3.14	51.0 ± 16.4	22.2 ± 9.9
FAT [64]	$8.64 \pm 1.76 \pm 1.70 \pm 0.90$	48.0 ± 16.0	26.0 ± 8.6
Data	10.00 ± 0.50	49.7 ± 1.7	22.4 ± 1.5
$B_s^0 \rightarrow \phi \bar{K}^{*0}$	$0.12_{-0.03-0.03-0.04}^{+0.04+0.04+0.06}$	$74.5_{-4.8-3.7-6.4}^{+4.6+2.5+3.4}$	$12.7_{-2.5-1.8-1.8}^{+2.4+2.2+3.3}$
PQCD-I [60]	$0.65_{-0.13-0.18-0.04}^{+0.16+1.27+0.10}$	$71.2_{-3.0-3.7-0.0}^{+3.2+2.7+0.0}$	$13.3_{-1.5-1.3-0.0}^{+1.4+1.7+0.0}$
PQCD-II [62]	$0.39_{-0.17}^{+0.20}$	$50.0_{-7.2}^{+8.1}$	$24.2_{-3.9}^{+3.6}$
QCDF-I [38]	$0.4_{-0.1-0.3}^{+0.1+0.5}$	40_{-1-35}^{+1+67}	...
QCDF-II [61]	$0.37_{-0.05-0.20}^{+0.06+0.24}$	43_{-2-18}^{+2+21}	...
QCDF-III [95] ^a	$0.11_{-0.04-0.01}^{+0.07+0.06}$	$43.6_{-24.0-25.3}^{+14.6+51.5}$	$25.9_{-9.1-23.5}^{+8.4+14.4}$
SCET [63]	0.56 ± 0.19	54.6 ± 15.0	20.5 ± 9.1
FAT [64]	$0.70 \pm 0.11 \pm 0.13 \pm 0.08$	38.9 ± 14.7	31.4 ± 8.1
Data	1.14 ± 0.30	51.0 ± 17.0	...
$B^+ \rightarrow \phi K^{*+}$	$7.6_{-1.8-1.1-1.8}^{+2.9+1.4+2.8}$	$72.3_{-3.9-2.6-0.5}^{+4.4+2.9+2.2}$	$14.3_{-2.2-1.6-1.2}^{+1.9+1.2+0.1}$
PQCD-I [52]	15.96	74.8	11.1
PQCD-II [62]	$10.3_{-3.8}^{+4.9}$	$57.0_{-5.9}^{+6.3}$	$21.0_{-3.0}^{+3.0}$
QCDF-I [38]	$10.1_{-0.5-7.1}^{+0.5+12.2}$	45_{-0-36}^{+0+58}	...
QCDF-II [39]	$10.0_{-1.3-6.1}^{+1.4+12.3}$	49_{-42}^{+51}	25_{-25}^{+21}
SCET [63]	9.86 ± 3.39	51.0 ± 16.4	22.2 ± 9.9
FAT [64]	$9.31 \pm 1.90 \pm 1.83 \pm 0.97$	48.0 ± 16.0	25.9 ± 8.6
Data	10.0 ± 2.0	50.0 ± 5.0	20.0 ± 5.0

^aWe quote the results of Case II.

Since the width-to-mass ratio for ϕ and $K^*(892)$ are small, it is valid to apply the narrow width approximation for vector resonance to factorize the four-body process as three sequential two-body decays:

$$\mathcal{B}(B \rightarrow \phi(\rightarrow K\bar{K})K^*(\rightarrow K\pi)) \approx \mathcal{B}(B \rightarrow \phi K^*) \times \mathcal{B}(\phi \rightarrow K\bar{K}) \times \mathcal{B}(K^* \rightarrow K\pi), \quad (42)$$

for which we can extract the two-body $B \rightarrow \phi K^*$ branching ratios to compare with the current available predictions

and experiments. The longitudinal, perpendicular, and parallel polarization fractions of the P -wave amplitudes are defined as

$$f_0 = \frac{\mathcal{B}_0}{\mathcal{B}_P}, \quad f_{\parallel} = \frac{\mathcal{B}_{\parallel}}{\mathcal{B}_P}, \quad f_{\perp} = \frac{\mathcal{B}_{\perp}}{\mathcal{B}_P}, \quad (43)$$

with $\mathcal{B}_P = \mathcal{B}_0 + \mathcal{B}_{\parallel} + \mathcal{B}_{\perp}$ being the total P -wave branching ratio. The numerical results together with other theoretical results from PQCD [52, 60, 62], QCDF [38, 39, 61, 95], SCET [63] and FAT [64] are summarized in Table V for comparison. The world average values are taken from PDG [37] whenever available.

We see that the various approaches as well as experiment have similar branching ratios in magnitude for the B^0 and B^+ modes but quite different results for $\mathcal{B}(B_s^0 \rightarrow \phi \bar{K}^{*0})$. The predicted central values span a wide range: $(1.1 - 7.0) \times 10^{-7}$, which are generally below the current world average of $(1.14 \pm 0.30) \times 10^{-6}$. Our result is consistent with the recent QCDF calculation [95], and closer to the predictions from Refs. [38, 61, 62], but far from the previous PQCD value [60]. The discrepancy between theoretical predictions and experimental data remains an issue to be resolved.

According to the factorization assumption, the polarization fractions for the vector-vector modes should satisfy the naive counting rules [53]

$$f_0 \sim 1 - \mathcal{O}(m_V^2/M^2), \quad f_{\parallel} \sim f_{\perp} \sim \mathcal{O}(m_V^2/M^2), \quad (44)$$

with m_V being the vector meson mass. The longitudinal polarization is naively expected to be $f_0 \sim 0.9$ in $B \rightarrow \phi K^*$ decays. However, a low longitudinal polarization of order 0.5 has been observed in the $B \rightarrow \phi K^*$ decays by Belle [34, 35], BABAR [30–32], and LHCb [58, 59], which indicates a significant departure from the naive expectation of predominant longitudinal polarization and poses an interesting challenge for theoretical interpretations. Several attempts to understand the values of within or beyond the standard model have been made [38–51, 96–105].

In the PQCD approach, a large transverse polarization fraction derives from the weak annihilation diagram induced by the operator O_6 and nonfactorizable contributions [45]. However, the combined effects are not sufficient to reduce f_0 down to 0.5. As can be seen from Table V, our predictions for the longitudinal polarization fractions are generally larger than 0.7, agree with the previous PQCD calculations from Refs. [52, 60]. The small $f_0 \sim (0.50 - 0.57)$ in Ref. [62] is ascribed to the inclusion of the higher-power terms proportional to r^2 , with r being the mass ratio between the vector and B mesons. The QCDF [38, 39] and FAT [64] predictions on the longitudinal polarization fractions are generally less than 0.5. A recent Belle measurement [36] based on the Summer 2020 Belle II dataset of $34.6 fb^{-1}$, yield $f_0(B^0 \rightarrow \phi K^{*0}) = 0.57 \pm 0.20 \pm 0.04$ and $f_0(B^+ \rightarrow \phi K^{*+}) = 0.58 \pm 0.23 \pm 0.02$, to be compared with our results.

C. CP violating observables

TABLE VI: Direct CP asymmetries (in units of %) for the four-body $B^+ \rightarrow (K^+ K^-)(K^0 \pi^+)$ decay. The requirements on the $K\bar{K}$ and $K\pi$ invariant masses are $m_{\phi} - 0.015 < m_{K\bar{K}} < m_{\phi} + 0.015$ (GeV) and $m_{K^*} - 0.15 < m_{K\pi} < m_{K^*} + 0.15$ (GeV). The sources of theoretical errors are the same as in previous tables but added in quadrature.

\mathcal{A}_0^{CP}	$\mathcal{A}_{\parallel}^{CP}$	\mathcal{A}_{\perp}^{CP}	\mathcal{A}_{SS}^{CP}	\mathcal{A}_{VS}^{CP}	\mathcal{A}_{SV}^{CP}	$\mathcal{A}_{\text{total}}^{CP}$
$-4.1^{+6.1}_{-4.6}$	$5.8^{+2.1}_{-3.8}$	$4.9^{+3.8}_{-4.4}$	$4.5^{+2.0}_{-2.5}$	$3.8^{+2.2}_{-4.2}$	$3.2^{+0.1}_{-4.4}$	$-0.3^{+3.2}_{-2.5}$

TABLE VII: Theoretical predictions of CP violation (in %) for the $B^+ \rightarrow \phi K^{*+}$ decay in various approaches.

This work	Data [37]	PQCD [62]	QCDF [38]	QCDF [106]	SCET [63]	FAT [64]
$-1.5^{+4.9}_{-3.3}$	-1 ± 8	-1.0	0^{+0}_{-1}	0.05	-0.39 ± 0.44	1.00 ± 0.27

The direct CP asymmetry in each component and the overall asymmetry are defined as

$$\mathcal{A}_h^{CP} = \frac{\bar{\mathcal{B}}_h - \mathcal{B}_h}{\bar{\mathcal{B}}_h + \mathcal{B}_h}, \quad \mathcal{A}_{\text{total}}^{CP} = \frac{\sum_h \bar{\mathcal{B}}_h - \sum_h \mathcal{B}_h}{\sum_h \bar{\mathcal{B}}_h + \sum_h \mathcal{B}_h}, \quad (45)$$

respectively. Since only penguin operators work on the neutral channels, there is no direct CP asymmetry in the neutral B^0 and B_s^0 modes. However, the charged mode receives an additional tree contribution and the direct CP

asymmetries arises from the interference between the tree and penguin amplitudes. As shown in Table VI, the direct CP asymmetries for various helicity states turn out to be small, $\sim \mathcal{O}(10^{-2})$, and the overall CP asymmetry is even lower at the order of 10^{-3} . It can be understood as follows. The tree contribution only appears in the annihilation diagrams, which are power suppressed with respect to the emission ones. Furthermore, the CKM element $|V_{ub}^* V_{us}|$ of tree diagrams is smaller than $|V_{tb}^* V_{ts}|$ of penguin diagrams. Our result in Tables VI for the VS and SV components are consistent with the world averages of $(4 \pm 16)\%$ and $(-15 \pm 12)\%$ [37], respectively, within uncertainties.

In Table VII, we list the predicted direct CP asymmetry of the mode $B^+ \rightarrow \phi K^{*+}$ in PQCD. For comparison, the experimental data, as well as predictions from previous PQCD [62], QCDF [38, 106], SCET [63], and FAT [64], are also presented. All the theoretical approaches show that a nearly vanishing direct CP asymmetry, comply with the latest world average of -0.01 ± 0.08 [37] from the measurements [34, 107]

$$\mathcal{A}^{CP}(B^+ \rightarrow \phi K^{*+}) = \begin{cases} 0.00 \pm 0.09(\text{stat}) \pm 0.04(\text{syst}) & \text{BABAR,} \\ -0.02 \pm 0.14(\text{stat}) \pm 0.03(\text{syst}) & \text{Belle.} \end{cases}$$

Any observation of large direct CP asymmetry to this mode will be a signal for new physics.

TPAs, as mentioned in the Introduction, may be potential signals of CP violation, and thus are complementary to the direct CP violations, particularly when the latter are suppressed by the strong phase. According to Eq. (1), TPAs can be calculated from integrations of the differential decay rate as

$$\begin{aligned} A_T^1 &= \frac{\Gamma((2\zeta_1 - 1)(2\zeta_2 - 1) \sin \varphi > 0) - \Gamma((2\zeta_1 - 1)(2\zeta_2 - 1) \sin \varphi < 0)}{\Gamma((2\zeta_1 - 1)(2\zeta_2 - 1) \sin \varphi > 0) + \Gamma((2\zeta_1 - 1)(2\zeta_2 - 1) \sin \varphi < 0)} \\ &= -\frac{2\sqrt{2}}{\pi\mathcal{D}} \int d\omega_1 d\omega_2 k(\omega_1)k(\omega_2)k(\omega_1, \omega_2) \text{Im}[A_\perp A_0^*], \\ A_T^2 &= \frac{\Gamma(\sin(2\varphi) > 0) - \Gamma(\sin(2\varphi) < 0)}{\Gamma(\sin(2\varphi) > 0) + \Gamma(\sin(2\varphi) < 0)} \\ &= -\frac{4}{\pi\mathcal{D}} \int d\omega_1 d\omega_2 k(\omega_1)k(\omega_2)k(\omega_1, \omega_2) \text{Im}[A_\perp A_\parallel^*], \\ A_T^3 &= \frac{\Gamma((2\zeta_1 - 1) \sin \varphi > 0) - \Gamma((2\zeta_1 - 1) \sin \varphi < 0)}{\Gamma((2\zeta_1 - 1) \sin \varphi > 0) + \Gamma((2\zeta_1 - 1) \sin \varphi < 0)} \\ &= -\frac{3}{\sqrt{2}\mathcal{D}} \int d\omega_1 d\omega_2 k(\omega_1)k(\omega_2)k(\omega_1, \omega_2) \text{Im}[A_\perp A_{VS}^*], \\ A_T^4 &= \frac{\Gamma((2\zeta_2 - 1) \sin \varphi > 0) - \Gamma((2\zeta_2 - 1) \sin \varphi < 0)}{\Gamma((2\zeta_2 - 1) \sin \varphi > 0) + \Gamma((2\zeta_2 - 1) \sin \varphi < 0)} \\ &= -\frac{3}{\sqrt{2}\mathcal{D}} \int d\omega_1 d\omega_2 k(\omega_1)k(\omega_2)k(\omega_1, \omega_2) \text{Im}[A_\perp A_{SV}^*], \\ A_T^5 &= \frac{\Gamma(\sin \varphi > 0) - \Gamma(\sin \varphi < 0)}{\Gamma(\sin \varphi > 0) + \Gamma(\sin \varphi < 0)} \\ &= -\frac{9\pi}{4\sqrt{2}\mathcal{D}} \int d\omega_1 d\omega_2 k(\omega_1)k(\omega_2)k(\omega_1, \omega_2) \text{Im}[A_\perp A_{SS}^*], \end{aligned} \quad (46)$$

with

$$\mathcal{D} = \int d\omega_1 d\omega_2 k(\omega_1)k(\omega_2)k(\omega_1, \omega_2) \sum_h Y_h |A_h|^2, \quad (47)$$

where the mass integration extends over the chosen mass window. It is seen that the TPAs are produced by the interference between A_\perp and A_i with $i = 0, \parallel, SV, VS, SS$ and take the form $\text{Im}(A_\perp A_i^*) = |A_\perp| |A_i^*| \sin(\Delta\phi + \Delta\delta)$, where $\Delta\phi$ and $\Delta\delta$ respectively denote weak and strong phase differences between the two amplitudes. Here the strong phase difference could produce a nonzero value, even if the weak phases vanish. Thus, a nonzero TPA is not necessarily a signal of CP violation. In order to obtain a true signal of CP violation, one has to compare the TPAs in B and \bar{B} decays. The helicity amplitudes for the CP -conjugated process can be obtained by applying the following transformations

$$A_0 \rightarrow \bar{A}_0, A_\parallel \rightarrow \bar{A}_\parallel, A_\perp \rightarrow -\bar{A}_\perp, A_{SV} \rightarrow \bar{A}_{SV}, A_{VS} \rightarrow \bar{A}_{VS}, A_{SS} \rightarrow \bar{A}_{SS}. \quad (48)$$

Then, the associated TPAs for the charge-conjugate process, \bar{A}_T^i , are defined similarly. Now, we can construct the true and fake asymmetries by combining A_T^i and \bar{A}_T^i [3]

$$\begin{aligned} A_T^i(\text{ture}) &= \frac{1}{2}(A_T^i + \bar{A}_T^i) \propto \sin(\Delta\phi) \cos(\Delta\delta), \\ A_T^i(\text{fake}) &= \frac{1}{2}(A_T^i - \bar{A}_T^i) \propto \cos(\Delta\phi) \sin(\Delta\delta). \end{aligned} \quad (49)$$

It was pointed out in Ref. [9] that the second equation above are valid only in the absence of direct CP asymmetry in the total decay rate. As the total direct CP asymmetry does not exceed a few percent as shown in Table VI, above approximation holds in $B \rightarrow \phi K^*$ decays. It is clear that $A_T^i(\text{true})$ do not suffer the suppression from the strong phase $\Delta\delta$ compared with the direct CP violation. It is nonzero only if the weak phases are nonzero, and provides a measure for CP violation. Nevertheless, $A_T^i(\text{fake})$ can be nonzero even if the weak phases are zero. Such a quantity will sometimes be referred to as a fake asymmetry. It reflect the importance of strong final-state phases [9], thus is not a signal of CP violation. Since the helicity amplitudes always have different strong phases, this will lead to nonzero fake TPAs for all decays.

TABLE VIII: PQCD predictions for the TPAs(%). The mass of the $K\bar{K}(K\pi)$ pair is required to be within 15 MeV (150 MeV) of the known $\phi(K^*)$ meson mass.

Asymmetries	$B^0 \rightarrow (K^+K^-)(K^+\pi^-)$	$B_s^0 \rightarrow (K^+K^-)(K^-\pi^+)$	$B^+ \rightarrow (K^+K^-)(K^0\pi^+)$
A_T^1	$-13.8_{-4.3}^{+4.8}$	$-24.0_{-3.8}^{+6.6}$	$-14.1_{-3.8}^{+5.0}$
\bar{A}_T^1	$13.8_{-4.3}^{+4.8}$	$24.0_{-3.8}^{+6.6}$	$+13.8_{-3.9}^{+5.6}$
$A_T^1(\text{true})$	0.0	0.0	$-0.15_{-0.30}^{+0.05}$
$A_T^1(\text{fake})$	$-13.8_{-4.3}^{+4.8}$	$-24.0_{-3.8}^{+6.6}$	$-14.0_{-3.9}^{+5.3}$
A_T^2	$-0.3_{-0.1}^{+0.1}$	$-0.1_{-0.0}^{+0.0}$	$-0.3_{-0.1}^{+0.1}$
\bar{A}_T^2	$0.3_{-0.1}^{+0.1}$	$0.1_{-0.0}^{+0.0}$	$0.2_{-0.0}^{+0.1}$
$A_T^2(\text{true})$	0.0	0.0	$-0.05_{-0.05}^{+0.00}$
$A_T^2(\text{fake})$	$-0.3_{-0.1}^{+0.1}$	$-0.1_{-0.0}^{+0.0}$	$-0.3_{-0.1}^{+0.1}$
A_T^3	$-5.4_{-0.6}^{+1.0}$	$-6.4_{-2.2}^{+2.1}$	$-5.6_{-0.6}^{+1.0}$
\bar{A}_T^3	$5.4_{-0.6}^{+1.0}$	$6.4_{-2.2}^{+2.1}$	$5.5_{-0.6}^{+1.0}$
$A_T^3(\text{true})$	0.0	0.0	$-0.05_{-0.00}^{+0.00}$
$A_T^3(\text{fake})$	$-5.4_{-0.6}^{+1.0}$	$-6.4_{-2.2}^{+2.1}$	$-5.6_{-0.6}^{+1.0}$
A_T^4	$1.6_{-3.0}^{+3.0}$	$-8.1_{-3.3}^{+3.2}$	$1.6_{-2.7}^{+3.2}$
\bar{A}_T^4	$-1.6_{-3.0}^{+3.0}$	$8.1_{-3.3}^{+3.2}$	$-1.8_{-2.8}^{+3.1}$
$A_T^4(\text{true})$	0.0	0.0	$-0.10_{-0.00}^{+0.05}$
$A_T^4(\text{fake})$	$1.6_{-3.0}^{+3.0}$	$-8.1_{-3.3}^{+3.2}$	$1.7_{-2.8}^{+3.2}$
A_T^5	$-4.3_{-0.8}^{+1.1}$	$-6.7_{-1.9}^{+1.8}$	$-4.2_{-0.8}^{+1.1}$
\bar{A}_T^5	$4.3_{-0.8}^{+1.1}$	$6.7_{-1.9}^{+1.8}$	$4.3_{-0.8}^{+1.2}$
$A_T^5(\text{true})$	0.0	0.0	$0.05_{-0.05}^{+0.00}$
$A_T^5(\text{fake})$	$-4.3_{-0.8}^{+1.1}$	$-6.7_{-1.9}^{+1.8}$	$-4.3_{-0.8}^{+1.2}$

The calculated TPAs for the concerned decays are collected in Table VIII. In the special case of the involved neutral intermediate states $B^0 \rightarrow \phi K^{*0}$ and $B_s^0 \rightarrow \phi \bar{K}^{*0}$ modes, in which each helicity amplitude involves the same single weak phase in the SM. This results in $A_T^i = -\bar{A}_T^i$ due to the vanishing weak phase difference. The true TPAs for the two neutral modes are thus expected to be zero as shown in Table VIII. If such asymmetries are observed experimentally, it is probably a signal of new physics. The situation of the fake TPAs is different. Many non-zero and even sizable fake TPAs are predicted in our calculations. The magnitude of $A_T^1(\text{fake})$ for the B^0 and B^+ channels exceed ten percent, even reaching 24.0% for the B_s one, whereas the S -wave induced fake TPAs, $A_T^{3,4,5}(\text{fake})$, are predicted to be several percent. The smallness of $A_T^2(\text{fake})$ are caused by the suppression from the strong phase difference between the perpendicular and parallel polarization amplitudes, which are found to be very close to 0 in PQCD framework [60, 62]. Hence, the measurement of a large A_T^2 would point clearly towards the presence of new physics beyond the SM.

Experimentally, an complete angular analysis of the decay $B^0 \rightarrow \phi K^{*0}$ is available from LHCb [58], BABAR [31, 32], and Belle [34, 35] collaborations, which allows us to determine the true and fake TPAs from the measured polarization

TABLE IX: Comparison of measurements in the angular analysis of $B^0 \rightarrow \phi K^{*0}$ made by BABAR [32], Belle [35] and LHCb [58] experiments, where the first and second uncertainties are statistical and systematic, respectively. The true and fake TPAs (the last four entries) are deduced from the fitted parameters (the first eight lines).

Parameters	BABAR	Belle	LHCb
f_L	$0.494 \pm 0.034 \pm 0.013$	$0.499 \pm 0.030 \pm 0.018$	$0.497 \pm 0.019 \pm 0.015$
f_\perp	$0.212 \pm 0.032 \pm 0.013$	$0.238 \pm 0.026 \pm 0.008$	$0.221 \pm 0.016 \pm 0.013$
δ_\perp	$2.35 \pm 0.13 \pm 0.09$	$2.37 \pm 0.10 \pm 0.04$	$2.633 \pm 0.062 \pm 0.037$
δ_\parallel	$2.40 \pm 0.13 \pm 0.08$	$2.23 \pm 0.10 \pm 0.02$	$2.562 \pm 0.069 \pm 0.040$
A_0^{CP}	$+0.01 \pm 0.07 \pm 0.02$	$-0.030 \pm 0.061 \pm 0.007$	$-0.003 \pm 0.038 \pm 0.005$
A_\perp^{CP}	$-0.04 \pm 0.15 \pm 0.06$	$-0.14 \pm 0.11 \pm 0.01$	$+0.047 \pm 0.072 \pm 0.009$
δ_\perp^{CP}	$+0.21 \pm 0.13 \pm 0.08$	$+0.05 \pm 0.10 \pm 0.02$	$+0.062 \pm 0.062 \pm 0.006$
δ_\parallel^{CP}	$+0.22 \pm 0.12 \pm 0.08$	$-0.02 \pm 0.10 \pm 0.01$	$+0.045 \pm 0.068 \pm 0.015$
Asymmetries	BABAR	Belle	LHCb
$A_T^1(true)$	$-0.046 \pm 0.031 \pm 0.017$	$-0.029 \pm 0.025 \pm 0.005$	$-0.007 \pm 0.012 \pm 0.002$
$A_T^2(true)$	$-0.003 \pm 0.056 \pm 0.036$	$0.021 \pm 0.040 \pm 0.006$	$+0.004 \pm 0.014 \pm 0.002$
$A_T^1(fake)$	$-0.203 \pm 0.031 \pm 0.019$	$-0.211 \pm 0.025 \pm 0.010$	$-0.105 \pm 0.012 \pm 0.006$
$A_T^2(fake)$	$0.016 \pm 0.058 \pm 0.038$	$-0.041 \pm 0.040 \pm 0.013$	$-0.017 \pm 0.014 \pm 0.003$

TABLE X: Parameters measured in the angular analysis of $B^+ \rightarrow \phi K^{*+}$ by BABAR [107], where the first and second uncertainties are statistical and systematic, respectively. The true and fake TPAs (the last four entries) are deduced from the fitted parameters (the first eight lines).

Parameters	BABAR
f_L	$+0.49 \pm 0.05 \pm 0.03$
f_\perp	$+0.21 \pm 0.05 \pm 0.02$
$\delta_\perp - \pi$	$-0.45 \pm 0.20 \pm 0.03$
$\delta_\parallel - \pi$	$-0.67 \pm 0.20 \pm 0.07$
A_0^{CP}	$+0.17 \pm 0.11 \pm 0.02$
A_\perp^{CP}	$+0.22 \pm 0.24 \pm 0.08$
δ_\perp^{CP}	$+0.19 \pm 0.20 \pm 0.07$
δ_\parallel^{CP}	$+0.07 \pm 0.20 \pm 0.05$
Asymmetries	BABAR
$A_T^1(true)$	$-0.025 \pm 0.056 \pm 0.019$
$A_T^2(true)$	$0.028 \pm 0.084 \pm 0.026$
$A_T^1(fake)$	$-0.114 \pm 0.056 \pm 0.011$
$A_T^2(fake)$	$-0.061 \pm 0.084 \pm 0.023$

amplitudes, phases and amplitude differences between B^0 and \bar{B}^0 decays. Since the concerned decays are all self-tagged processes, whose triple product asymmetry can be computed separately for B and \bar{B} decays. We note that the definitions of the CP asymmetries and TPAs are different among these measurements. To compare these results directly, it is necessary to rescale them with the unified definitions. We follow the convention of Ref. [9], defining

$$\begin{aligned}
 (A_T^1)_{\text{exp}} &= -\frac{2\sqrt{2}}{\pi} \frac{\text{Im}(A_\perp A_0^*)}{|A_0|^2 + |A_\parallel|^2 + |A_\perp|^2}, \\
 (A_T^2)_{\text{exp}} &= -\frac{4}{\pi} \frac{\text{Im}(A_\perp A_\parallel^*)}{|A_0|^2 + |A_\parallel|^2 + |A_\perp|^2}.
 \end{aligned} \tag{50}$$

The corresponding quantities for the charge-conjugate process, $(\bar{A}_T^{1,2})_{\text{exp}}$, are defined similarly. We can calculate the true and fake asymmetries from Eq. (49). The measured polarizations, phases and CP violation asymmetries as well as the true and fake TPAs of $B^0 \rightarrow \phi K^{*0}$ by the LHCb, BABAR and Belle collaborations are compared in Table IX. One can see that all the true asymmetries are measured to be consistent with zero, showing no evidence for CP

violation. Nevertheless, a significant fake asymmetry, such as $A_T^1(fake)$, is observed in all three different experiments, reflect the importance of final-state interactions. The comparisons here are only for the P -wave components. The S -wave induced TPAs, arise from the interference between A_\perp and one S -wave amplitude, have not been determined in BABAR and Belle, since the contributions of S -wave $K\bar{K}$ and $K\pi$ and their interferences were not fully included into the angular analysis. It is pointed out that contributions from the S -wave $K\bar{K}$ and $K\pi$ are significant and should be taken into account in future measurements. The three additional CP -violating observables can then provide valuable complementary information on NP.

The only available amplitude analysis of $B^+ \rightarrow \phi K^{*+}$ was performed by BABAR [107] experiment. The fitted polarization parameters together with the true and fake TPAs are summarized in Table X. The S -wave $K\pi$ contribution was included to resolve the twofold phase ambiguity, but the accurate assessments of the S -wave component have not been determined, leading to the corresponding S -wave induced TPAs are still absent.

Although the polarization fractions and branching ratio of the decay $B_s^0 \rightarrow \phi \bar{K}^{*0}$ have been measured by the LHCb experiment [59], the full angular analysis has not been done because of the limited signal events, which results in the measurement on TPAs are not yet available. As indicated in Table VIII, the predicted large fake TPAs for the B_s mode would be tested in the future.

IV. CONCLUSION

B meson four-body decays provide a wealth of information on the weak interactions, in terms of a number of observables ranging from the branching ratios, polarizations, CP asymmetries, and triple product asymmetries to a full angular analysis. In this work, we have concentrated on the penguin-dominated $B_{(s)} \rightarrow \phi(\rightarrow K\bar{K})K^*(\rightarrow K\pi)$ decays using the perturbative QCD approach. The calculations were performed in the $K\bar{K}(K\pi)$ invariant mass window of 15(150) MeV around the $\phi(K^*)$ mass. In addition to the dominant vector resonances, four-particle final states can also be obtained through one or two scalar meson intermediate states in the given mass regions. The strong dynamics of the scalar or vector resonance decays into the meson pair was parametrized into the corresponding two-meson DAs, which has been well established in three-body B meson decays. Angular momentum conservation in the decay allows for three amplitudes for vector-vector decays and one single amplitude in modes involving at least one scalar $K\bar{K}(K\pi)$ pair. The CP -averaged branching ratios of all components were predicted in the chosen mass ranges. The single S -wave contributions were found to be significant and consistent with the data from the LHCb experiment, while the double S -wave contributions were only a few percent in the considered invariant mass range. It has been demonstrated that the S -wave contributions were strongly sensitive to the integrating ranges. After choosing the same $K\pi$ mass range, our results can be comparable with the Belle and BABAR measurements roughly.

We extracted the two-body $B \rightarrow \phi K^*$ branching ratios from the results for the corresponding quasi-two-body modes by employing the narrow width approximation. The obtained results basically agree with previous predictions performed in the two-body framework within theoretical uncertainty. However, various predictions for $\mathcal{B}(B_s^0 \rightarrow \phi \bar{K}^{*0})$ lie in a wide range, generally below the current world average value. The gap between theory and experiment requires a more thorough study. The longitudinal polarization fractions were estimated to be $f_0 \sim 0.7$, somewhat lower than the naive expectation of a dominant longitudinal polarization because of the important chirally enhanced annihilation and nonfactorizable contributions. However, the observation of an even smaller value of 0.5 by Belle, BABAR, and LHCb, means the existing explanations of the abnormal polarization are not satisfactory and thus calling for more in-depth studies.

We have also investigated the direct CP asymmetries and TPAs in the $B \rightarrow (K\bar{K})(K\pi)$ decays. For the two pure-penguin neutral channels, both the direct CP asymmetries and true TPAs should be zero in SM due to the vanishing weak phase difference. It was observed that the direct CP asymmetries for the charged modes are small, of order 10^{-2} , since the tree contribution are significantly suppressed compared to the penguin ones. A similar observation were made in previous PQCD, QCDF, SCET, and FAT approaches and supported by the measurements from BABAR and Belle. The true TPAs are predicted to be tiny, of order 10^{-3} , compatible with the absence of CP violation. Whereas, the fake TPAs were found to be sizable, which can provide valuable information on final-state interactions.

The full angular analysis of $B^0 \rightarrow \phi K^{*0}$ have been performed by LHCb, BABAR, and Belle experiments, allow one to derive the true and fake TPAs from the results of the angular analysis. It is worth noting that the S -wave components and their interference have not been fully considered into the analysis in BABAR and Belle experiments. Therefore, the only available measurements for the S -wave induced TPAs are from LHCb. By including the S -wave $K\bar{K}$ and $K\pi$ components, we have estimated the S -wave induced TPAs for the first time. The predicted asymmetries $B^0 \rightarrow \phi K^{*0}$ are in good agreement with those reported by the LHCb. As the three additional CP -violating observables may provide valuable complementary information on NP, a dedicated angular analysis from Belle and BABAR data is expected. The full angular analysis of $B_s^0 \rightarrow \phi \bar{K}^{*0}$ was still not available due to the limited samples. The obtained asymmetries can be confronted with the future data.

Experimental measurement may be improved by expanding the mass region to around 1.5 GeV based on more precise data in the future. Then the angular analysis could include the contributions of some higher excited intermediate states, such as D -wave $K_2^*(1430)$, P -wave $\phi(1680)$, and S -wave $f_0(1370)$, and so on. The additional contributions and their interferences would provide a lot of meaningful asymmetries in angular distributions, lead to the amplitude analysis will be more complicate and complete. This is an intriguing topic for future investigation.

Acknowledgments

This work is supported by National Natural Science Foundation of China under Grant Nos. 12075086, 12005103 and 11605060. ZR is supported in part by the Natural Science Foundation of Hebei Province under Grant Nos. A2021209002 and A2019209449. YL is also supported by the Natural Science Foundation of Jiangsu Province under Grant No. BK20190508 and the Research Start-up Funds of Nanjing Agricultural University.

Appendix A: Decay Amplitudes

Here we present the helicity amplitudes for the concerned channels as following

$$\begin{aligned}
\mathcal{A}_h(B^0 \rightarrow \phi(\rightarrow K^+K^-)K^{*0}(\rightarrow K^+\pi^-)) &= \frac{G_F}{\sqrt{2}} V_{tb}^* V_{ts} X_h \left\{ \frac{4}{3} \left[C_3 + C_4 - \frac{1}{2}(C_9 + C_{10}) \right] \mathcal{F}_e^{LL} \right. \\
&+ \left[C_5 + \frac{1}{3}C_6 - \frac{1}{2}(C_7 + \frac{1}{3}C_8) \right] \mathcal{F}_e^{LR} \\
&+ \left[C_6 + \frac{1}{3}C_5 - \frac{1}{2}(C_8 + \frac{1}{3}C_7) \right] \mathcal{F}_e^{SP} \\
&+ \left[C_3 + C_4 - \frac{1}{2}(C_9 + C_{10}) \right] \mathcal{M}_e^{LL} \\
&+ (C_5 - \frac{1}{2}C_7) \mathcal{M}_e^{LR} + (C_6 - \frac{1}{2}C_8) \mathcal{M}_e^{SP} \\
&+ \left[C_4 + \frac{1}{3}C_3 - \frac{1}{2}(C_{10} + \frac{1}{3}C_9) \right] \mathcal{F}_a^{LL} \\
&+ \left[C_6 + \frac{1}{3}C_5 - \frac{1}{2}(C_8 + \frac{1}{3}C_7) \right] \mathcal{F}_a^{SP} \\
&\left. + (C_3 - \frac{1}{2}C_9) \mathcal{M}_a^{LL} + (C_5 - \frac{1}{2}C_7) \mathcal{M}_a^{LR} \right\}, \tag{A1}
\end{aligned}$$

$$\begin{aligned}
\mathcal{A}_h(B_s^0 \rightarrow \phi(\rightarrow K^+K^-)\bar{K}^{*0}(\rightarrow K^-\pi^+)) &= \frac{G_F}{\sqrt{2}} V_{tb}^* V_{td} X_h \left\{ \left[C_3 + \frac{1}{3}C_4 - \frac{1}{2}(C_9 + \frac{1}{3}C_{10}) \right] \mathcal{F}_e^{LL} \right. \\
&+ \left[C_4 + \frac{1}{3}C_3 - \frac{1}{2}(C_{10} + \frac{1}{3}C_9) \right] \mathcal{F}'_e^{LL} \\
&+ \left[C_6 + \frac{1}{3}C_5 - \frac{1}{2}(C_8 + \frac{1}{3}C_7) \right] \mathcal{F}'_e^{SP} \\
&+ \left[C_5 + \frac{1}{3}C_6 - \frac{1}{2}(C_7 + \frac{1}{3}C_8) \right] \mathcal{F}_e^{LR} \\
&+ (C_4 - \frac{1}{2}C_{10}) \mathcal{M}_e^{LL} + (C_3 - \frac{1}{2}C_9) \mathcal{M}'_e^{LL} \\
&+ (C_6 - \frac{1}{2}C_8) \mathcal{M}_e^{SP} + (C_5 - \frac{1}{2}C_7) \mathcal{M}'_e^{LR} \\
&+ \left[C_4 + \frac{1}{3}C_3 - \frac{1}{2}(C_{10} + \frac{1}{3}C_9) \right] \mathcal{F}'_a^{LL} \\
&+ \left[C_6 + \frac{1}{3}C_5 - \frac{1}{2}(C_8 + \frac{1}{3}C_7) \right] \mathcal{F}'_a^{SP} \\
&\left. + (C_3 - \frac{1}{2}C_9) \mathcal{M}'_a^{LL} + (C_5 - \frac{1}{2}C_7) \mathcal{M}_a^{LR} \right\}, \tag{A2}
\end{aligned}$$

$$\begin{aligned}
\mathcal{A}_h(B^+ \rightarrow \phi(\rightarrow K^+K^-)K^{*+}(\rightarrow K^0\pi^+)) &= \frac{G_F}{\sqrt{2}}V_{ub}^*V_{us}X_h \left\{ (C_2 + \frac{1}{3}C_1)\mathcal{F}_a^{LL} + (C_1)\mathcal{M}_a^{LL} \right\} \\
&- \frac{G_F}{\sqrt{2}}V_{tb}^*V_{ts}X_h \left\{ \frac{4}{3} \left[C_3 + C_4 - \frac{1}{2}(C_9 + C_{10}) \right] \mathcal{F}_e^{LL} \right. \\
&+ \left[C_5 + \frac{1}{3}C_6 - \frac{1}{2}(C_7 + \frac{1}{3}C_8) \right] \mathcal{F}_e^{LR} \\
&+ \left[C_6 + \frac{1}{3}C_5 - \frac{1}{2}(C_8 + \frac{1}{3}C_7) \right] \mathcal{F}_e^{SP} \\
&+ \left[C_3 + C_4 - \frac{1}{2}(C_9 + C_{10}) \right] \mathcal{M}_e^{LL} \\
&+ (C_5 - \frac{1}{2}C_7)\mathcal{M}_e^{LR} + (C_6 - \frac{1}{2}C_8)\mathcal{M}_e^{SP} \\
&+ \left[C_4 + \frac{1}{3}C_3 + C_{10} + \frac{1}{3}C_9 \right] \mathcal{F}_a^{LL} \\
&+ \left[C_6 + \frac{1}{3}C_5 + C_8 + \frac{1}{3}C_7 \right] \mathcal{F}_a^{SP} \\
&\left. + (C_3 + C_9)\mathcal{M}_a^{LL} + (C_5 + C_7)\mathcal{M}_a^{LR} \right\}, \tag{A3}
\end{aligned}$$

with

$$X_h = \begin{cases} \sqrt{1+4\alpha_1}\sqrt{1+4\alpha_2}, & h = 0, \parallel, \perp \\ \sqrt{1+4\alpha_{1,2}}, & h = SV, VS \\ 1, & h = SS. \end{cases} \tag{A4}$$

The explicit expressions of \mathcal{F}/\mathcal{M} can be found in [15]. Note that the term \mathcal{F}_e^{SP} from the operators O_{5-8} vanishes when a vector resonance is emitted from the weak vertex, because neither the scalar nor the pseudoscalar density gives contributions to the vector resonance production.

-
- [1] N. Sinha and R. Sinha, Determination of the angle gamma using $B \rightarrow D^*V$ modes, Phys. Rev. Lett. **80**, 3706 (1998).
 - [2] G. Kramer and W. F. Palmer, Branching ratios and CP asymmetries in the decay $B \rightarrow VV$, Phys. Rev. D **45**, 193 (1992).
 - [3] E. Kou *et al.* (Belle II Collaboration), The Belle-II Physics Book, PTEP **2019**, 123C01 (2019) [erratum: PTEP **2020**, 029201 (2020)].
 - [4] S. Stone and L. Zhang, S-waves and the Measurement of CP Violating Phases in B_s Decays, Phys. Rev. D **79**, 074024 (2009).
 - [5] Y. Xie, P. Clarke, G. Cowan and F. Muheim, Determination of $2\beta_s$ in $B_s^0 \rightarrow J/\psi K^+K^-$ decays in the presence of a K^+K^- S-wave contribution, JHEP **09**, 074 (2009).
 - [6] B. Bhattacharya, A. Datta, M. Duraisamy and D. London, Searching for new physics with $\bar{b} \rightarrow \bar{s} B_s^0 \rightarrow V_1V_2$ penguin decays, Phys. Rev. D **88**, 016007 (2013).
 - [7] W. Bensalem and D. London, T odd triple product correlations in hadronic b decays, Phys. Rev. D **64**, 116003 (2001).
 - [8] A. Datta and D. London, Triple-product correlations in $B \rightarrow V_1V_2$ decays and new physics, Int. J. Mod. Phys. A **19**, 2505 (2004).
 - [9] M. Gronau and J. L. Rosner, Triple product asymmetries in K , $D_{(s)}$ and $B_{(s)}$ decays, Phys. Rev. D **84**, 096013 (2011).
 - [10] A. Datta, M. Duraisamy and D. London, Searching for New Physics with B-Decay Fake Triple Products, Phys. Lett. B **701**, 357 (2011).
 - [11] A. Datta, M. Duraisamy and D. London, New Physics in $b \rightarrow s$ Transitions and the $B_{d,s}^0 \rightarrow V_1V_2$ Angular Analysis, Phys. Rev. D **86**, 076011 (2012).
 - [12] S. K. Patra and A. Kundu, CPT violation and triple-product correlations in B decays, Phys. Rev. D **87**, 116005 (2013).
 - [13] G. Durieux and Y. Grossman, Probing CP violation systematically in differential distributions, Phys. Rev. D **92**, 076013 (2015).
 - [14] A. J. Bevan, C, P, and CP asymmetry observables based on triple product asymmetries, arXiv:1408.3813 [hep-ph].
 - [15] Z. Rui, Y. Li, and H. n. Li, Four-body decays $B_{(s)} \rightarrow (K\pi)_{S/P}(K\pi)_{S/P}$ in the perturbative QCD approach, J. High Energy Phys. **05** (2021) 082.
 - [16] Y. Li, D. C. Yan, Z. Rui and Z. J. Xiao, Study of $B_{(s)} \rightarrow (\pi\pi)(K\pi)$ decays in the perturbative QCD approach, Eur. Phys. J. C **81**, 806 (2021).

- [17] W. F. Wang, H. n. Li, W. Wang and C. D. Lü, S -wave resonance contributions to the $B_{(s)}^0 \rightarrow J/\psi\pi^+\pi^-$ and $B_s \rightarrow \pi^+\pi^-\mu^+\mu^-$ decays, Phys. Rev. D **91**, 094024 (2015).
- [18] S. Kräinkl, T. Mannel and J. Virto, Three-body non-leptonic B decays and QCD factorization, Nucl. Phys. B **899**, 247 (2015).
- [19] D. Boito, J. P. Dedonder, B. El-Bennich, R. Escribano, R. Kaminski, L. Lesniak and B. Loiseau, Parametrizations of three-body hadronic B - and D -decay amplitudes in terms of analytic and unitary meson-meson form factors, Phys. Rev. D **96**, 113003 (2017).
- [20] A. G. Grozin, On wave functions of meson pairs and meson resonances, Sov. J. Nucl. Phys. **38** (1983) 289.
- [21] A. G. Grozin, One- and two-particle wave functions of multihadron systems, Theor. Math. Phys. **69** (1986) 1109.
- [22] D. Müller, D. Robaschik, B. Geyer, F.-M. Dittes, and J. Hořejši, Wave functions, evolution equations and evolution kernels from light ray operators of QCD, Fortschr. Physik. **42** (1994) 101.
- [23] M. Diehl, T. Gousset, B. Pire and O. Teryaev, Probing partonic structure in $\gamma^*\gamma \rightarrow \pi\pi$ near threshold, Phys. Rev. Lett. **81** (1998) 1782.
- [24] M. Diehl, T. Gousset and B. Pire, Exclusive production of pion pairs in $\gamma^*\gamma$ collisions at large Q^2 , Phys. Rev. D **62** (2000) 073014.
- [25] B. Pire and L. Szymanowski, Impact representation of generalized distribution amplitudes, Phys. Lett. B **556** (2003) 129.
- [26] M.V. Polyakov, Hard exclusive electroproduction of two pions and their resonances, Nucl. Phys. **B555** (1999) 231.
- [27] C. H. Chen and H. n. Li, Three body nonleptonic B decays in perturbative QCD, Phys. Lett. B **561** (2003) 258.
- [28] R. A. Briere *et al.* (CLEO Collaboration), Observation of $B \rightarrow \phi K$ and $B \rightarrow \phi K^*$, Phys. Rev. Lett. **86**, 3718 (2001).
- [29] B. Aubert *et al.* (BaBar Collaboration), Rates, polarizations, and asymmetries in charmless vector-vector B meson decays, Phys. Rev. Lett. **91**, 171802 (2003).
- [30] B. Aubert *et al.* (BaBar Collaboration), Measurement of the $B^0 \rightarrow \phi K^0$ decay amplitudes, Phys. Rev. Lett. **93**, 231804 (2004).
- [31] B. Aubert *et al.* (BaBar Collaboration), Vector-tensor and vector-vector decay amplitude analysis of $B^0 \rightarrow \phi K^{*0}$, Phys. Rev. Lett. **98**, 051801 (2007).
- [32] B. Aubert *et al.* (BaBar Collaboration), Time-Dependent and Time-Integrated Angular Analysis of $B \rightarrow \phi K_S^0 \pi^0$ and $B \rightarrow \phi K^\pm \pi^\mp$, Phys. Rev. D **78**, 092008 (2008).
- [33] K. F. Chen *et al.* (Belle Collaboration), Measurement of branching fractions and polarization in $B \rightarrow \phi K^{(*)}$ decays, Phys. Rev. Lett. **91**, 201801 (2003).
- [34] K. F. Chen *et al.* (Belle Collaboration), Measurement of polarization and triple-product correlations in $B \rightarrow \phi K^*$ decays, Phys. Rev. Lett. **94**, 221804 (2005).
- [35] M. Prim *et al.* (Belle Collaboration), Angular analysis of $B^0 \rightarrow \phi K^*$ decays and search for CP violation at Belle, Phys. Rev. D **88**, 072004 (2013).
- [36] F. Abudinén *et al.* (Belle-II Collaboration), Rediscovery of $B \rightarrow \phi K^{(*)}$ decays and measurement of the longitudinal polarization fraction f_L in $B \rightarrow \phi K^*$ decays using the Summer 2020 Belle II dataset, arXiv:2008.03873 [hep-ex].
- [37] Particle Data Group, Review of particle physics, Prog. Theor. Exp. Phys. **2020**, 083C01 (2020).
- [38] M. Beneke, J. Rohrer and D. Yang, Branching fractions, polarisation and asymmetries of $B \rightarrow VV$ decays, Nucl. Phys. B **774**, 64-101 (2007).
- [39] H. Y. Cheng and K. C. Yang, Branching Ratios and Polarization in $B \rightarrow VV, VA, AA$ Decays, Phys. Rev. D **78**, 094001 (2008) [erratum: Phys. Rev. D **79**, 039903 (2009)].
- [40] Y. Grossman, Beyond the standard model with B and K physics, Int. J. Mod. Phys. A **19**, 907-917 (2004).
- [41] P. K. Das and K. C. Yang, Data for polarization in charmless $B \rightarrow \phi K^*$: A Signal for new physics?, Phys. Rev. D **71**, 094002 (2005).
- [42] C. H. Chen and C. Q. Geng, Scalar interactions to the polarizations of $B \rightarrow \phi K^*$, Phys. Rev. D **71**, 115004 (2005).
- [43] Y. D. Yang, R. M. Wang and G. R. Lu, Polarizations in decays $B_{u,d} \rightarrow VV$ and possible implications for R-parity violating SUSY, Phys. Rev. D **72**, 015009 (2005).
- [44] A. L. Kagan, Polarization in $B \rightarrow VV$ decays, Phys. Lett. B **601**, 151-163 (2004).
- [45] H. n. Li and S. Mishima, Polarizations in $B \rightarrow VV$ decays, Phys. Rev. D **71**, 054025 (2005).
- [46] M. Beneke, J. Rohrer and D. Yang, Enhanced electroweak penguin amplitude in $B \rightarrow VV$ decays, Phys. Rev. Lett. **96**, 141801 (2006).
- [47] A. Datta, A. V. Gritsan, D. London, M. Nagashima and A. Szykman, Testing Explanations of the $B \rightarrow \phi K^*$ Polarization Puzzle, Phys. Rev. D **76**, 034015 (2007).
- [48] C. W. Bauer, D. Pirjol, I. Z. Rothstein and I. W. Stewart, $B \rightarrow M_1 M_2$: Factorization, charming penguins, strong phases, and polarization, Phys. Rev. D **70**, 054015 (2004).
- [49] P. Colangelo, F. De Fazio and T. N. Pham, The Riddle of polarization in $B \rightarrow VV$ transitions, Phys. Lett. B **597**, 291-298 (2004).
- [50] M. Ladisa, V. Laporta, G. Nardulli and P. Santorelli, Final state interactions for $B \rightarrow VV$ charmless decays, Phys. Rev. D **70**, 114025 (2004).
- [51] H. Y. Cheng, C. K. Chua and A. Soni, Final state interactions in hadronic B decays, Phys. Rev. D **71**, 014030 (2005).
- [52] C. H. Chen, Y. Y. Keum and H. n. Li, Perturbative QCD analysis of $B \rightarrow \phi K^*$ decays, Phys. Rev. D **66**, 054013 (2002).
- [53] H. n. Li, Resolution to the $B \rightarrow \phi K^*$ polarization puzzle, Phys. Lett. B **622**, 63 (2005).
- [54] W. S. Hou and M. Nagashima, Resolving the $B \rightarrow \phi K^*$ polarization anomaly, arXiv:hep-ph/0408007 [hep-ph].
- [55] W. j. Zou and Z. j. Xiao, The Charmless $B \rightarrow PV, VV$ decays and new physics effects in the mSUGRA model, Phys.

- Rev. D **72**, 094026 (2005).
- [56] Q. Chang, X. Q. Li and Y. D. Yang, Constraints on the anomalous tensor operators from $B \rightarrow \phi K^*, \eta K^*$, and ηK decays, JHEP **06**, 038 (2007).
- [57] S. S. Bao, F. Su, Y. L. Wu and C. Zhuang, Exclusive $B \rightarrow VV$ Decays and CP Violation in the General two-Higgs-doublet Model, Phys. Rev. D **77**, 095004 (2008).
- [58] R. Aaij *et al.* (LHCb Collaboration), Measurement of polarization amplitudes and CP asymmetries in $B^0 \rightarrow \phi K^*(892)^0$, JHEP **05**, 069 (2014).
- [59] R. Aaij *et al.* (LHCb Collaboration), First observation of the decay $B_s^0 \rightarrow \phi \bar{K}^{*0}$, JHEP **11**, 092 (2013).
- [60] A. Ali, G. Kramer, Y. Li, C. D. Lu, Y. L. Shen, W. Wang and Y. M. Wang, Charmless non-leptonic B_s decays to PP , PV and VV final states in the pQCD approach, Phys. Rev. D **76**, 074018 (2007).
- [61] H. Y. Cheng and C. K. Chua, QCD Factorization for Charmless Hadronic B_s Decays Revisited, Phys. Rev. D **80**, 114026 (2009).
- [62] Z. T. Zou, A. Ali, C. D. Lu, X. Liu and Y. Li, Improved Estimates of The $B_{(s)} \rightarrow VV$ Decays in Perturbative QCD Approach, Phys. Rev. D **91**, 054033 (2015).
- [63] C. Wang, S. H. Zhou, Y. Li and C. D. Lu, Global Analysis of Charmless B Decays into Two Vector Mesons in Soft-Collinear Effective Theory, Phys. Rev. D **96**, 073004 (2017).
- [64] C. Wang, Q. A. Zhang, Y. Li and C. D. Lu, Charmless $B_{(s)} \rightarrow VV$ Decays in Factorization-Assisted Topological-Amplitude Approach, Eur. Phys. J. C **77**, 333 (2017).
- [65] D. C. Yan, X. Liu and Z. J. Xiao, Anatomy of $B_s \rightarrow VV$ decays and effects of next-to-leading order contributions in the perturbative QCD factorization approach, Nucl. Phys. B **935**, 17 (2018).
- [66] Z. Rui, Y. Li and H. Li, Studies of the resonance components in the B_s decays into charmonia plus kaon pair, Eur. Phys. J. C **79**, 792 (2019).
- [67] Y. Li, D. C. Yan, J. Hua, Z. Rui and H. n. Li, Global determination of two-meson distribution amplitudes from three-body B decays in the perturbative QCD approach, Phys. Rev. D **104**, 096014 (2021).
- [68] S. Cheng, A. Khodjamirian, and J. Virto, Timelike-helicity $B \rightarrow \pi\pi$ form factor from light-cone sum rules with dipion distribution amplitudes, Phys. Rev. D **96** (2017) 051901(R).
- [69] C. Hambrook, and A. Khodjamirian, Form factors in $\bar{B}^0 \rightarrow \pi^+ \pi^0 l \bar{\nu}_l$ from QCD light-cone sum rules, Nucl. Phys. **B905** (2016) 373.
- [70] H.-Y. Cheng, C.-K. Chua, and K.-C. Yang, Charmless hadronic B decays involving scalar mesons: Implications on the nature of light scalar mesons, Phys. Rev. D **73**, 014017 (2006).
- [71] H.-Y. Cheng, C.-K. Chua, and K.-C. Yang, Charmless B decays to a scalar meson and a vector meson, Phys. Rev. D **77**, 014034 (2008).
- [72] M. K. Jia, C. Q. Zhang, J. M. Li and Z. Rui, S-wave contributions to the $B_{(s)} \rightarrow \chi_{c1}(\pi\pi, K\pi, KK)$ decays, Phys. Rev. D **104**, 073001 (2021).
- [73] D. Aston *et al.* (LASS Collaboration), Nucl. Phys. **B296**, 493 (1988).
- [74] R. Aaij *et al.* (LHCb Collaboration), Amplitude analysis of $B^0 \rightarrow \bar{D}^0 K^+ \pi^-$ decays, Phys. Rev. D **92** (2015) 012012.
- [75] S. M. Flatte, On the Nature of 0^+ Mesons, Phys. Lett. B **63**, 228-230 (1976).
- [76] R. Aaij *et al.* (LHCb Collaboration), Measurement of resonant and CP components in $\bar{B}_s^0 \rightarrow J/\psi \pi^+ \pi^-$ decays, Phys. Rev. D **89**, 092006 (2014).
- [77] D. V. Bugg, Reanalysis of data on $a_0(1450)$ and $a_0(980)$, Phys. Rev. D **78**, 074023 (2008).
- [78] Y. Li, Z. Rui, and Z.J. Xiao, P -wave contributions to $B_{(s)} \rightarrow \psi K \pi$ decays in perturbative QCD approach, Chin. Phys. C **44** (2020) 073102.
- [79] Y. Li, D. C. Yan, Z. Rui, Z.-J. Xiao, S , P and D -wave resonance contributions to $B_{(s)} \rightarrow \eta_c(1S, 2S) K \pi$, Phys. Rev. D **101** (2020) 016015.
- [80] H. n. Li, QCD aspects of exclusive B meson decays, Prog. Part. Nucl. Phys. **51**, 85 (2003).
- [81] T. Kurimoto, H. n. Li and A. I. Sanda, Leading power contributions to $B \rightarrow \pi$, rho transition form-factors, Phys. Rev. D **65**, 014007 (2002).
- [82] J. Hua, H. n. Li, C. D. Lu, W. Wang and Z. P. Xing, Global analysis of hadronic two-body B decays in the perturbative QCD approach, Phys. Rev. D **104**, 016025 (2021).
- [83] W. Wang, Y. M. Wang, J. Xu, and S. Zhao, B -meson light-cone distribution amplitude from the Euclidean quantity, Phys. Rev. D **102**, 011502(R) (2020).
- [84] H. n. Li and H. S. Liao, B meson wave function in k_T factorization, Phys. Rev. D **70**, 074030 (2004).
- [85] H. n. Li, Y. L. Shen, and Y. M. Wang, Resummation of rapidity logarithms in B meson wave functions, J. High Energy Phys. **02** (2013) 008.
- [86] H. n. Li and Y. M. Wang, Non-dipolar Wilson links for transverse-momentum-dependent wave functions, J. High Energy Phys. **06** (2015) 013.
- [87] H. n. Li, Y. L. Shen, and Y. M. Wang, Next-to-leading-order corrections to $B \rightarrow \pi$ form factors in k_T factorization, Phys. Rev. D **85**, 074004 (2012).
- [88] Y. K. Hsiao, and C. Q. Geng, Four-body baryonic decays of $B \rightarrow p \bar{p} \pi^+ \pi^- (\pi^+ K^-)$ and $\Lambda \bar{p} \pi^+ \pi^- (\pi^+ K^-)$, Phys. Lett. B **770** (2017) 348.
- [89] C. s. Kim, Y. Li and W. Wang, Study of Decay Modes $B \rightarrow K_0^*(1430) \phi$, Phys. Rev. D **81**, 074014 (2010).
- [90] J. P. Lees *et al.* (BaBar Collaboration), B^0 meson decays to $\rho^0 K^{*0}$, $f_0 K^{*0}$, and $\rho^- K^{*+}$, including higher K^* resonances, Phys. Rev. D **85**, 072005 (2012).
- [91] S. H. Kyeon *et al.* (Belle Collaboration), Measurements of Charmless Hadronic $b \rightarrow s$ Penguin Decays in the $\pi^+ \pi^- K^+ \pi^-$

- Final State and Observation of $B^0 \rightarrow \rho^0 K^+ \pi^-$, Phys. Rev. D **80**, 051103 (2009).
- [92] M. Ablikim *et al.* (BES Collaboration), Partial wave analysis of $\chi_{c0} \rightarrow \pi^+ \pi^- K^+ K^-$, Phys. Rev. D **72**, 092002 (2005).
- [93] H. Y. Cheng, C. W. Chiang and C. K. Chua, Finite-Width Effects in Three-Body B Decays, Phys. Rev. D **103**, 036017 (2021).
- [94] H. Y. Cheng, C. W. Chiang and C. K. Chua, Width effects in resonant three-body decays: B decay as an example, Phys. Lett. B **813**, 136058 (2021).
- [95] Q. Chang, X. Li, X. Q. Li and J. Sun, Study of the weak annihilation contributions in charmless $B_s \rightarrow VV$ decays, Eur. Phys. J. C **77**, 415 (2017).
- [96] E. Alvarez, L. N. Epele, D. Gomez Dumm and A. Szykman, Right handed currents and FSI phases in $B^0 \rightarrow \phi K^{*0}$, Phys. Rev. D **70**, 115014 (2004).
- [97] K. C. Yang, Annihilation in factorization-suppressed B decays involving a 1^1P_1 meson and search for new-physics signals, Phys. Rev. D **72**, 034009 (2005) [erratum: Phys. Rev. D **72**, 059901 (2005)].
- [98] S. Baek, A. Datta, P. Hamel, O. F. Hernandez and D. London, Polarization states in $B \rightarrow \rho K^*$ and new physics, Phys. Rev. D **72**, 094008 (2005).
- [99] C. S. Huang, P. Ko, X. H. Wu and Y. D. Yang, MSSM anatomy of the polarization puzzle in $B \rightarrow \phi K^*$ decays, Phys. Rev. D **73**, 034026 (2006).
- [100] C. H. Chen and H. Hatanaka, Nonuniversal Z-prime couplings in B decays, Phys. Rev. D **73**, 075003 (2006).
- [101] A. Faessler, T. Gutsche, J. C. Helo, S. Kovalenko and V. E. Lyubovitskij, On the possible resolution of the B-meson decay polarization anomaly in R-parity violating SUSY, Phys. Rev. D **75**, 074029 (2007).
- [102] C. H. Chen, C. Q. Geng, Y. K. Hsiao and Z. T. Wei, Productions of $K_0^*(1430)$ and K_1 in B decays, Phys. Rev. D **72**, 054011 (2005).
- [103] C. H. Chen and C. Q. Geng, Expectations on $B \rightarrow (K_0^*(1430), K_2^*(1430))\phi$ decays, Phys. Rev. D **75**, 054010 (2007).
- [104] H. Y. Cheng and K. C. Yang, Charmless Hadronic B Decays into a Tensor Meson, Phys. Rev. D **83**, 034001 (2011).
- [105] C. Bobeth, M. Gorbahn and S. Vickers, Weak annihilation and new physics in charmless $B \rightarrow MM$ decays, Eur. Phys. J. C **75**, 340 (2015).
- [106] H. Y. Cheng and C. K. Chua, Revisiting Charmless Hadronic $B_{u,d}$ Decays in QCD Factorization, Phys. Rev. D **80**, 114008 (2009).
- [107] B. Aubert *et al.* (BaBar Collaboration), Amplitude Analysis of the $B^\pm \rightarrow \phi K^*(892)^\pm$ Decay, Phys. Rev. Lett. **99**, 201802 (2007).